

**Effect of Temperature, Concentration of Precursors and Distance
between Precursors on the synthesis of Molybdenum Disulfide
(MoS₂) using Chemical vapor Deposition (CVD) technique – CVD
grown monolayer MoS₂ based RRAM**

A Dissertation

SUBMITTED IN PARTIAL FULFILLMENT OF THE REQUIREMENTS

FOR THE AWARD OF THE DEGREE

OF

MASTER OF SCIENCE

IN

PHYSICS

Submitted by :

Satakshi Pandey (2k19/MSCPHY/05)

Aparna (2k19/MSCPHY/21)

Under the supervision of

Dr Bharti Singh



Department of Applied Physics

Delhi Technological University

Bawana Road, Delhi – 110042

MAY, 2021

Department of Applied Physics

CONTENTS

Cover Page
Candidate's Declaration
Plagiarism
Acceptance
Registration
Acknowledgement
Abstract
Contents
List of Figures
List of Tables
List of Symbols, abbreviations

CHAPTER 1: INTRODUCTION

1.1 Two-dimensional Materials – Introduction to Transition Metal Dichalcogenides (TMDCs).
1.2 Classification of Semiconductor Memory
1.3 Significance of this work

CHAPTER 2: LITERATURE REVIEW

2.1 Research Trends in the advancement of MoS₂
2.2 Research Trends in 2D MoS₂ based RRAM

CHAPTER 3: Synthesis of MoS₂ using Chemical vapor Deposition (CVD) technique

3.1 CVD technique for synthesis of Molybdenum DiSulphide (MoS₂)
3.2 Experimental Setup for Synthesis of MoS₂
3.3 Thermal Deposition of Silver Electrodes
3.4 Device fabrication and electrical measurement.
3.5 Conduction mechanism of the MoS₂ based RRAM device

CHAPTER 4: RESULT AND DISCUSSION

4.1 Characterization
4.1.1 Optical Spectroscopy
4.1.2 Raman Spectroscopy
4.1.3. Photoluminescence Spectroscopy
4.2 Fabricated monolayer MoS₂ based RRAM Device
4.3 Experimental Results- Effect of Variation of parameters on the growth of MoS₂.
4.4 Transfer characteristics of prepared RRAM (Ag/MoS₂/Ag) Device

CHAPTER 5: CONCLUSION AND FUTURE SCOPE

5.1 Conclusion
5.2 Future Scope

REFERENCES

RESEARCH PAPER

DELHI TECHNOLOGICAL UNIVERSITY

(Formerly Delhi College of Engineering)

Bawana Road, Delhi-110042

CANDIDATE'S DECLARATION

We, **Satakshi Pandey(2k19/MSCPHY/05)** and **Aparna(2k19/MSCPHY/21)**, students of M.Sc. Physics, hereby declare that the project Dissertation titled "**Effect of Temperature, Concentration of Precursors and Distance between Precursors on synthesis of Molybdenum Disulfide (MoS₂) using Chemical vapor Deposition (CVD) technique – CVD grown monolayer MoS₂ based RRAM**" which is submitted by us to the Department of Applied Physics, Delhi Technological University, Delhi is original and not copied from any source without proper citation. This work has not previously formed the basis for the award of any Degree, Diploma Associateship, Fellowship or other similar title or Delhi Technological University, Delhi in partial fulfillment of the requirement for the award of the degree of Master of Science, is original and not copied from any source without proper citation. This work has not previously formed the basis for the award of any Degree, Diploma Associateship, Fellowship or other similar title or recognition. The work has been published accepted communicated in SCI/SCI expanded/SSCI/Scopus indexed journal or Peer reviewed scopus indexed conference with the following details:-

Title of Paper 1 - “Effect of Temperature, Precursor’s concentration and Distance between precursors on the synthesis of Molybdenum Disulfide (MoS₂) using Chemical vapour Deposition (CVD) technique” .

Author Names: Aparna, Satakshi Pandey, Dr Bharti Singh

Name of Conference: International Conference on Energy and Environment (ICEE-2021).

Conference Date: April 09-10, 2021.

Status of Paper : Published

Date of Paper communication: 25 March, 2021

Date of Paper Accepted: 12 April, 2021

Date of Paper Published: 9 May, 2021

Title of Paper 2 - “Chemical Vapor Deposition grown monolayer MoS₂ based Resistive Random Access Memory Device”.

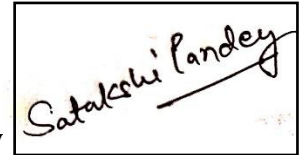
Author Names: Satakshi Pandey, Aparna, Dr Bharti Singh

Name of Conference: 6th International Conference on Advanced Production and Industrial Engineering (ICAPIE -2021)

Conference Date: April 09-10, 2021.
Status of Paper : Accepted
Date of Paper communication: 25 April,2021
Date of Paper Accepted: 13 May,2021
Date of Paper Published: October, 2021

Place: Delhi

Satakshi Pandey

A rectangular box containing a handwritten signature in black ink that reads "Satakshi Pandey".

Date: 31/05/2021

Aparna

A rectangular box containing a handwritten signature in blue ink that reads "Aparna".

DEPARTMENT OF APPLIED PHYSICS

DELHI TECHNOLOGICAL UNIVERSITY

(Formerly Delhi College of Engineering)

Bawana Road, Delhi-110042

CERTIFICATE

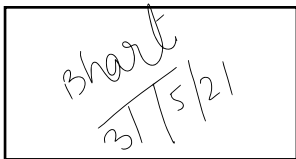
I hereby certify that the Project Dissertation titled "**Effect of Temperature, Concentration of Precursors and Distance between Precursors on synthesis of Molybdenum Disulfide (MoS₂) using Chemical vapor Deposition (CVD) technique – CVD grown monolayer MoS₂ based RRAM**" which is submitted by Satakshi Pandey(2k19/MSCPHY/05) and Aparna(2k19/MSCPHY/21), Department of Applied Physics, Delhi Technological University, Delhi in partial fulfillment of the requirement for the award of the degree of Master of Science, is a record of the project work carried out by the students under my supervision. To the best of my knowledge this work has not been submitted in part or full for any Degree or Diploma to this University or elsewhere.

Place: Delhi

Date: 31/05/2021

Dr. Bharti Singh

SUPERVISOR SIGN



Bharti
31/5/21

PLAGIARISM REPORT



Forplagcheck.docx
May 30, 2021
6209 words / 33549 characters

Forplagcheck.docx

Sources Overview

8%

OVERALL SIMILARITY

1	www.tandfonline.com INTERNET	3%
2	YingTao Li. "An overview of resistive random access memory devices", Chinese Science Bulletin, 10/2011 CROSSREF	<1%
3	Zusong Zhu, Dequan Zhu, Jie Zhang, Guisheng Jiang, Mingfang Yi, Jun Wen. "Optical thickness identification of few-layer MoS deposited b... CROSSREF	<1%
4	arxiv.org INTERNET	<1%
5	www.freepatentsonline.com INTERNET	<1%
6	Jiaqi Zhang, Wubo Li. "Chapter 8 Perovskite Materials for Resistive Random Access Memories", IntechOpen, 2020 CROSSREF	<1%
7	"Emerging Trends in Electrical, Communications, and Information Technologies", Springer Science and Business Media LLC, 2020 CROSSREF	<1%
8	aip.scitation.org INTERNET	<1%
9	Muhammad Muqet Rehman, Hafiz Mohammad Mutee Ur Rehman, Jahan Zeb Gul, Woo Young Kim, Khasan S Karimov, Nisar Ahmed. "Dec... CROSSREF	<1%
10	iopscience.iop.org INTERNET	<1%

11	www.frontiersin.org INTERNET	<1%
12	Chandreyee Manas Das, Qingling Ouyang, Lixing Kang, Yan Guo, Xuan-Quyen Dinh, Philippe Coquet, Ken-Tye Yong. "Augmenting sensitivity ... CROSSREF	<1%
13	Chulho Jung. "RESISTIVE SWITCHING AND THRESHOLD CURRENT OF Cr-DOPED SrTiO3 THIN FILMS DEPOSITED BY PULSED LASER DEP... CROSSREF	<1%
14	Deepti Chaudhary, Sandeep Munjal, Neeraj Khare, V.D. Vankar. "Bipolar resistive switching and nonvolatile memory effect in poly (3-hexylthi... CROSSREF	<1%
15	digital.lib.washington.edu INTERNET	<1%
16	A.L. Tan, S.S. Ng, H.A. Hassan. "Influence of sulfurization temperature on the molybdenum disulfide thin films grown by thermal vapour sul... CROSSREF	<1%
17	Deng, Donna D, Zhong Lin, Ana Laura Elías et al. "Electric-Field-Assisted Directed Assembly of Transition Metal Dichalcogenide Monolayer ... CROSSREF	<1%

30/05/2021

Forlagcheck.docx

18	Shih-Chen Shi. "Tribological Performance of Green Lubricant Enhanced by Sulfidation IF-MoS2", Materials, 2016 CROSSREF	<1%
19	Xiumei Zhang, Haiyan Nan, Shaoqing Xiao, Xi Wan, Zhenhua Ni, Xiaofeng Gu, Kostya Ostrikov. "Shape-Uniform, High-Quality Monolayered ... CROSSREF	<1%
20	repository.tudelft.nl INTERNET	<1%

Excluded search repositories:

- Submitted Works
- Crossref Posted Content

Excluded from Similarity Report:

- Bibliography
- Quotes
- Small Matches (less than 9 words).

Excluded sources:

- None

Bhart
31/5/21

PUBLICATION/ACCEPTANCE RECORD



Jyothi Engineering College

NAAC Accredited College with NBA Accredited Programmes*

Approved by AICTE & affiliated to APJ Abdul Kalam Technological University
A CENTRE OF EXCELLENCE IN SCIENCE & TECHNOLOGY BY THE CATHOLIC ARCHDIOCESE OF TRICHUR
JYOTHI HILLS, VETIKATTIRI P.O., CHERUTHURUTHY, TRISSUR, PIN-679531 Ph: +91-4884-259000, 274423 FAX: 04884-274777



NBA accredited B.Tech Programmes in Computer Science & Engineering, Electronics & Communication Engineering, Biotech & Bioscience Engineering and Mechanical Engineering valid for the academic year 2016-2022. NBA accredited B.Tech Programme in Civil Engineering valid for the academic year 2017-2022.



International Conference on Energy and Environment (ICEE 2021) April 09-10, 2021.

CERTIFICATE

This is to certify that the following paper has been presented and published in the International Conference on Energy and Environment (ICEE 2021 - Virtual Conference) during April 09-10, 2021 organized by Jyothi Engineering College, Thrissur, Kerala, India in association with Indian Society for Technical Education (ISTE).

Title of the Paper : Effect of Temperature, Precursors concentration and Distance between precursors on the synthesis of Molybdenum Disulfide (MoS₂) using Chemical Vapor Deposition (CVD) technique.

Author(s) : Aparna; Satakshi Pandey; Dr. Bharti Singh

Presented by : Aparna ; Satakshi Pandey



Rev. Fr. Roy Vadakkan
Chairman ICEE 2021



Dr. Sunny Joseph Kalayathankal
General Chair ICEE 2021



Dr. Deepanraj B.
Organizing Secretary ICEE 2021



Certificate

Dear Author(s): Satakshi Pandey, Aparna Aparna and Bharti Singh

Paper ID: 367

Paper Title: Chemical Vapor Deposition grown monolayer MoS₂ based Resistive Random Access Memory Device

This is to enlighten you that the above manuscript has been appraised by the editors of LNME and is accepted for the **6th International Conference on Advanced Production and Industrial Engineering (ICAPIE)- 2021 to be held during June 18-19, 2021**. The paper is recommended for publication in **Lecture Notes in Mechanical Engineering (Scopus Indexed publication of Springer Nature), ISSN: 2195-4356**. The manuscript has been submitted to Springer in May 2021 and will be online during October 2021.

Finally, the team of CAPIER DTU and ICAPIE-2021 would like to extend congratulations to you.



Prof. Ranganath M Singari
(Conference Chair, ICAPIE-2021)



Dr. Harish Kumar
(Convener, ICAPIE-2021)

REGISTRATION RECORD

PAPER 1

Fwd: ICEE 2021 Certificate of Presentation Inbox x



2K19/MSCPHY/21 APARNA <aparna_2k19mscphy21@dtu.ac.in>
to me ▾

7 May 2021, 18:41



----- Forwarded message -----

From: <icee@jecc.ac.in>
Date: Fri, May 7, 2021, 17:26
Subject: ICEE 2021 Certificate of Presentation
To: <aparna_2k19mscphy21@dtu.ac.in>

Dear Sir/Madam,

Thank you very much for your active participation in the "International Conference on Energy and Environment (ICEE 2021)" Organised by Department of Mechanical and Civil Engineering, Jyothi Engineering College in association with ISTE-JECC Chapter on April 09-10, 2021.

Herewith attached your presentation certificate. Sorry for the delay. Because of the COVID-19 pandemic, we are working from home and so it got delayed.

Thank you once again and we expect your cooperation and support in our future events.

With Regards

ICEE 2021 Team

Publications

All abstracts accepted and registered in International Conference on Energy and Environment will be published in Conference Proceedings.

Full length papers with plagiarism below 20% will be considered for publication in Scopus and SCI journals after peer review as per the publisher policy.

PAPER 2

----- Forwarded message -----

From: ICAPIE DTU <icapie.dtu@gmail.com>
Date: Thu, 13 May 2021 at 5:09 PM
Subject: Certificate of ICAPIE-2021 Paper ID: 367
To: <bhartisingh@dtu.ac.in>

Dear Author(s),

Please find attached the certificate of your paper accepted in ICAPIE-2021, which will be published in Lecture Notes in Mechanical Engineering, a Scopus Indexed publication of Springer.

Thanks for your support to ICAPIE-2021.

--

With Regards

Prof. Ranganath M Singari

Conference Chair
ICAPIE - 2021

Email- icapie.dtu@gmail.com

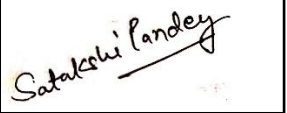
ACKNOWLEDGEMENT

We would like to express our thanks to our supervisor Dr Bharti Singh for providing us with the opportunity to work under her guidance and taking out time from her hectic schedule to assist with this dissertation. We would also like to thank the PhD scholars Vishal Singh, Shilpa Rana and Komal Singh for their constant support.

We would like to vouchsafe our substantial gratitude towards all faculty members at the Department of Applied Physics, Delhi Technological University.

We acknowledge with a deep sense of gratitude, the encouragement, cooperation, keen interest and inspiration received from all who have contributed to this work.

Satakshi Pandey



Aparna Department of Applied Physics



ABSTRACT

Graphene is a semimetal with zero bandgap which has imposed a limit on its applications in field-effect transistors and optoelectronics. Owing to this fact, other 2D materials such as h-BN, MXenes, phosphorene, and TMDCs were explored for their potential use in various electronic devices. Two-dimensional (2D) Transition Metal Dichalcogenides (TMDCs) have been engrossing a broad range of scientific interests due to their outstanding properties. Transition metal dichalcogenides (TMDCs) show excellent optical, mechanical, and electronic properties because they have a bandgap that is tunable and they exhibit a transition from indirect to direct bandgaps. Among all the explored TMDCs, MoS₂ has been eyeing the most attention. In the present study, monolayer MoS₂ has been grown on Si/SiO₂ substrate using the Chemical Vapor Deposition (CVD) technique, where MoO₃ and sulfur were used as the precursor. We analysed the tractable growth of monolayer MoS₂ developing to continuous films from triangular flakes by optimizing several parameters. The sample was further studied using various characterization techniques viz. Optical Spectroscopy, Raman Spectroscopy and Photoluminescence spectroscopy which showed that monolayer MoS₂ can be fabricated on Si/SiO₂ substrate by maintaining the temperature at 750°C for 15 to 30 minutes. The two distinctive Raman frequencies of E_{2g}¹ and A_{1g} vary persistently with the number of layers of ultrathin MoS₂ flakes, whereas the intensity and width of peaks vary inconsistently. Molybdenum disulfide (MoS₂) is one of the most quintessential TMDCs with a 1.84 eV direct bandgap in monolayer form which makes it scientifically as well as industrially important. Monolayer MoS₂ shows intense photoluminescence because of the quantum confinement effect. We have further studied the switching characteristics of the CVD-grown monolayer MoS₂ based RRAM device. Silver electrodes were deposited on the grown sample to form a planar MIM structure i.e., Ag/MoS₂/Ag. The typical I-V characteristics of the fabricated metal-insulator-metal (MIM) structure were studied using the two-probe measurement technique.

LIST OF TABLES

Table 1: Comparison of Bulk and Monolayer MoS₂.

Table 2: Summary of various synthesis techniques.

Table 3: Summary of MoS₂-based RRAM device.

Table 4: Effect of Concentration of Precursors.

Table 5: Effect of Distance between Boats containing Precursors.

Table 6: Effect of Temperature of the central zone of CVD.

LIST OF FIGURES

Fig.1.1: Crystal structure of monolayer MoS₂

Fig.1.2: Types of Semiconductor memories for storage of data.

Fig.1.3: Advantages of 2D MoS₂ based RRAM.

Fig.2.1: Different MoS₂ synthesis techniques.

Fig.2.2: Device structure Typical I–V curve of a MoO_x/MoS₂ memristor studied by Bessonov et al.

Fig.2.3: Device structure and material characterization image. Simplified view of the device structure signal transmission of monolayer MoS₂ based RF switches.

Fig.2.4: Schematic diagram of (a) Ag/MoS₂/Ag switch and (b) Fabrication process of MoS₂–UCNPs-based RRAM device.

Fig.3.1: Diagrammatic representation of Single Zone CVD Setup.

Fig.3.2: Profile of furnace temperature vs. Time of process.

Fig. 3.3: Diagrammatic representation of thermal evaporation method.

Fig.3.4: Electrical measurement and diagrammatic side view configurations of MoS₂ based memory device with Ag contacts.

Fig. 3.5: Depicts the CF-type conduction mechanism in Ag/MoS₂/Ag device.

Fig.3.6 (a) : shows the current-voltage characteristics of devices with unipolar switching.

Fig.3.6 (b): shows the current-voltage characteristics of devices with bipolar switching.

Fig. 4.1: Images showing a continuous thin film of MoS₂ grown on Si/SiO₂ substrate.

Fig. 4.2: Raman of MoS₂ thin film layer on SiO₂ /Si showing the region with prominent E_{2g}¹ and A^{1g} peaks.

Fig.4.3: Photoluminescence spectra of CVD-grown monolayer MoS₂.

Fig. 4.4(a): linear plot for the same two-probe transfer characteristics for a typical Ag/MoS₂/Ag device. The voltage was swept in the sequence of 0 V → 7V → 0 V → -7 V → 0 V, as shown by the coloured arrows with the four sweeps labelled as 1, 2, 3 and 4.

Fig 4.4(b): semi-logarithmic plot for the same two-probe transfer characteristics for a typical Ag/MoS₂/Ag device.

Fig. 5.1: Future prospect of 2D-materials based RRAM devices.

LIST OF SYMBOLS, ABBREVIATIONS

Abbreviation	Full form
TMDC	Transition metal dichalcogenides
2D	Two-dimensional
MoS₂	Molybdenum Disulfide
CVD	Chemical vapor deposition
RRAM	Resistive Random-Access Memory
NVM	Non-volatile Memory
MIM	Metal-Insulator-Metal
LRS	Low resistance state
HRS	High resistance state
PL	Photo-luminescence
ALD	Atomic layer deposition
PVD	Physical layer deposition
FTO	Fluorine-doped tin oxide
FET	Field effect Transistor
DI	De-ionized water
CMOS	Complementary metal oxide semiconductor
LDOS	Local density of states
RS	Resistance Switching

CHAPTER 1

INTRODUCTION

1.1 Two-dimensional (2D) materials

A class of materials known as two-dimensional (2D) materials, having a paramount limit of thinness constitute the thinnest artificial materials present in the universe. They have displayed themselves as a prolific ground for the discovery of remarkable phenomena in condensed matters and as a favourable platform to drive the boundaries of semiconductor technology beyond Moore's law.

Examples of 2D materials - Graphene and hexagonal boron nitrides, Phosphorene, MXenes, Transition Metal Dichalcogenides (TMDCs).

TMDCs such as WS_2 , MoS_2 , WSe_2 and $MoSe_2$ have a semiconductor bandgap due to which they are a promising candidate for future logic and memory devices beyond graphene[1]. Transition metal dichalcogenides (known as TMDCs) possess the chemical formula MX_2 . M is a transition metal (such as tungsten (W), molybdenum (Mo)) and X is a chalcogen (such as selenium (Se), Tellurium (Te) or sulfur (S)). TMDCs consists of a metal layer present in between two chalcogen layers[2].

Transition metal dichalcogenides (TMDs), two-dimensional (2D) atomic crystals have gained immense recent interest due to their potential applications and unique properties. They show a transition from indirect to direct bandgap which results in considerable intensification of photoluminescence[3]. Owing to these characteristics various researchers started exploring approaches for the synthesis of 2D TMDCs which included chemical exfoliation, liquid-phase exfoliation, micromechanical cleavage, and chemical vapour deposition (CVD). CVD method has been reported as the best technique for the growth of wafer-scale high-quality crystal films.

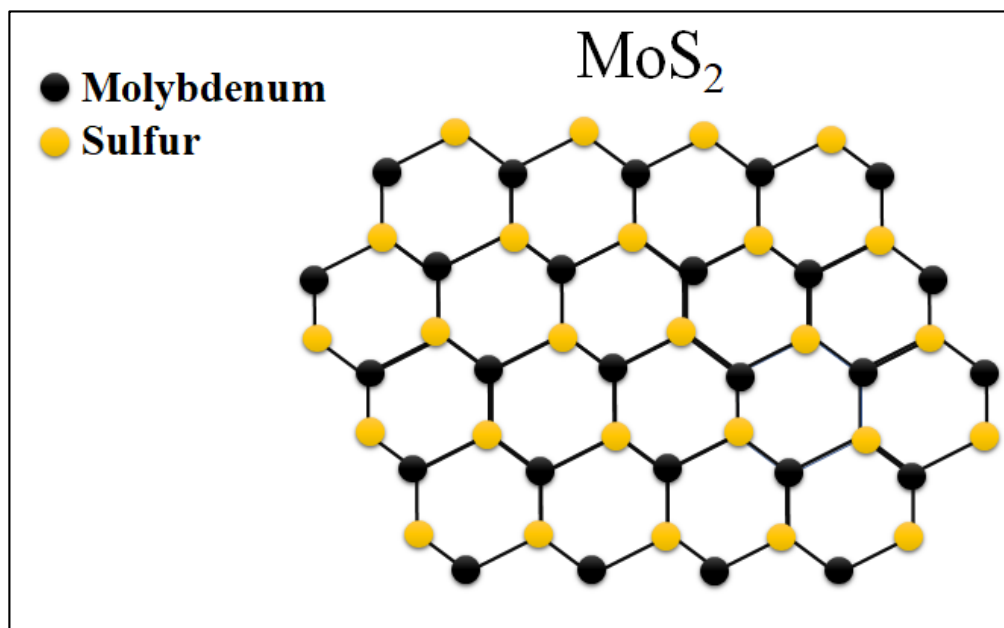


Fig.1.1: Crystal structure of monolayer MoS_2

MoS₂ was the next 2-dimensional material after graphene to be explored for its application in potential device applications including field-effect transistors and optical sensors. This interest arouses due to the transition into the direct bandgap from the indirect bandgap when the number of layers were reduced to monolayer form[4]. In the crystal structure of MoS₂, a hexagonal plane of Mo atoms has the hexagonal plane of S atoms present on either side. Mo and S atoms have covalent bonds present in between them whereas a weak van der Waals force holding layers together which allows the layers to be mechanically separated. The weak interaction between layers also allows the use of MoS₂ as a lubricant since the sheets can easily slide over one another. MoS₂ appears as a dark, shiny solid in the bulk layer form[5].

MoS₂ monolayer has a 1.84 eV direct bandgap, while the bulk layer of MoS₂ has an indirect bandgap at 1.2 eV. Monolayer MoS₂ show n-type behaviour having carrier mobilities approximately 350 cm² V⁻¹s⁻¹ which is approximately 500 times lower than graphene. But when they are used in the fabrication of FETs, they can display high on/off ratios up to 10⁸ which makes them fascinating for logic circuits and high-efficiency switching[6].

The semiconductor memory is classified into RAM and ROM. In ROM, only reading of data is allowed while in RAM data can be written into memory as well as read from memory. RAMs are further classified into volatile memories and nonvolatile memories based on the retention of stored data. Nonvolatile memories (NVM) store information even after the power is turned off while Volatile memories lose the stored data once the power is removed which happens in dynamic random-access memory (DRAM) and static random access memory (SRAM)[7].

1.2 Classification of Semiconductor Memory

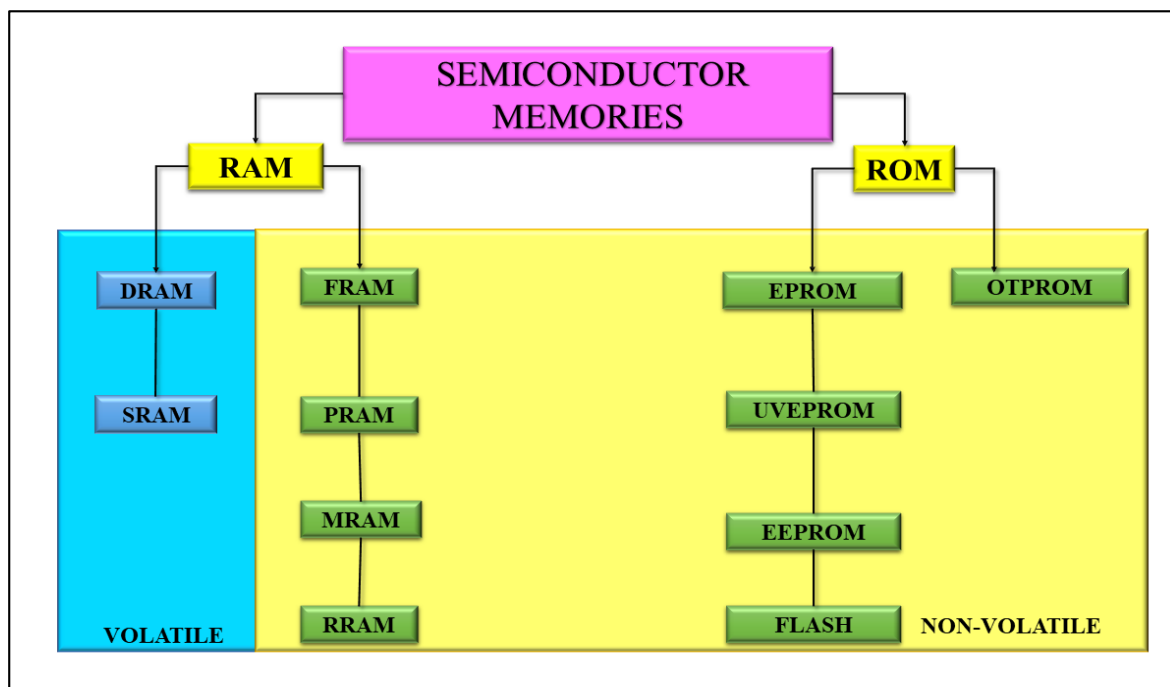


Fig. 1.2 : Types of Semiconductor memories for storage of data.

DRAM is volatile and requires to be refreshed every few seconds which raises the power consumption though they offer high density and high capacity. On the other hand, volatile SRAMs are fast but have large memory cell which reduces capacity. Flash memory which is non-volatile is also very famous for its high capacity but has the drawback that it is relatively slow. Researchers are constantly looking for new technologies which can satisfy all requirements. The characteristics of an ideal memory include fast response, high capacity, low power consumption, and long retention time.

Recently, NVM memories such as magnetic random access memory (MRAM), phase-change random access memory (PRAM), ferroelectric random access memory (FRAM), and resistive random access memory (RRAM)[8] have been zealously studied. Among all, RRAM has been advantageous for memory applications because of its fast switching, excellent scalability, easy fabrication, high integration density, good compatibility with CMOS technology, simple structure. RRAM show switching between a low resistance state (LRS) and a high resistance state(HRS).

RRAM is composed of a resistive material or insulating material present in between two conductive electrodes forming a metal-insulator-metal (MIM) structure. The MIM structure can transition between a high-resistance state (HRS or logic 0) and a low-resistance state (LRS or logic 1) by applying an appropriate voltage. Retention time operating speed, resistance ratio, operating voltage, device yield, endurance, device yield, and multilevel storage are important performance parameters of RRAM. The most important advantages offered by RRAM devices based on 2D materials include high electrical endurance voltage fast switching speed and extended mechanical robustness[6].

Resistive switching hysteretic behaviour has been observed in many materials under the application of the electric field. This dissertation presents the fabrication technologies, device structures, conduction mechanisms, resistive switching properties, challenges and future aspects of monolayer MoS₂ -based RRAMs.

1.3 Significance of this work

The objective of this thesis is to establish authentic methods for the growth of high-quality monolayer MoS₂ and its characterization for memory-based applications. This thesis is organized as follows: Chapter 2 offers an overview of the literature review. Chapter 3 illustrates the synthesis of MoS₂ using the Chemical Vapour Deposition (CVD) Technique. Optical Spectroscopy, Raman Spectroscopy and, Photoluminescence spectroscopy are employed to characterize the CVD-grown monolayer MoS₂. Chapter 4 demonstrates the Fabrication of MoS₂ based Resistive Random-Access Memory (RRAM) Device.

Chapter 5. provides a summary and results of our work. Chapter 6. shows the future work for improving the performance of TMD based RRAM and for further study of 2D MoS₂ characterizations and engineering.

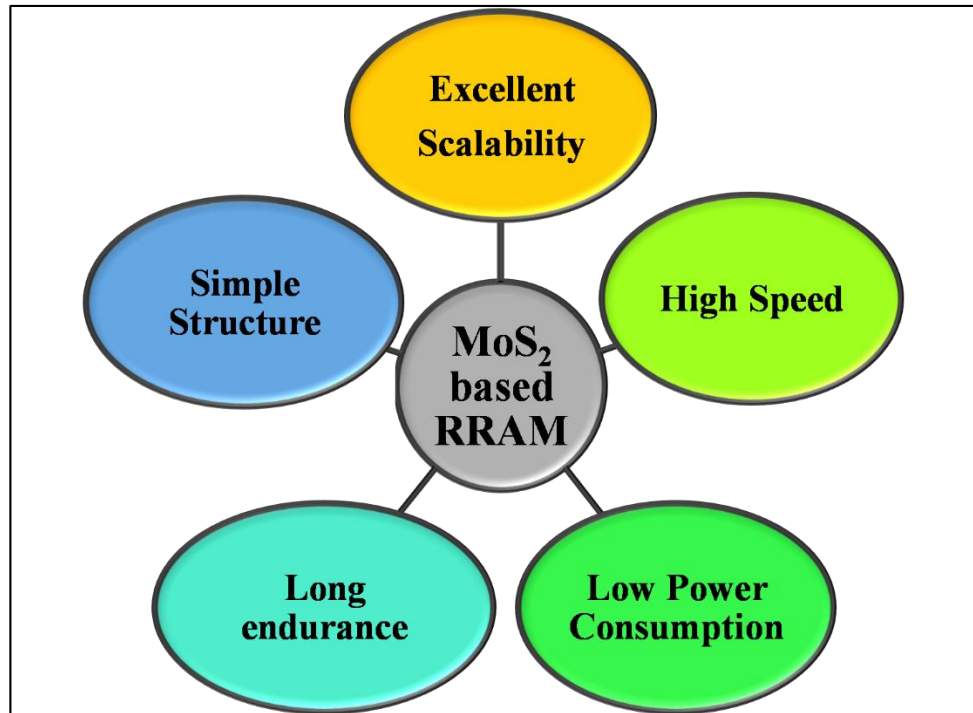


Fig. 1.3: Advantages of 2D MoS₂ based RRAM.

CHAPTER 2

LITERATURE REVIEW

2.1 Research Trends in the advancement of synthesis of MoS₂:

In the 1990s, carbon nanotube was found to be favourable material for the electronic applications and photovoltaic devices. But due to there inadequacy to differ from metal phase to semiconducting phase, researchers started to look for a better alternative. 2D-materials like graphene and TMDCs like WS₂, WS₂, MoS₂ and MoSe₂ caught attention of researchers because of there two dimensional structure. Properties of Graphene like high thermal conductivity and no band gap lead it to find application in low power electronic devices. But absence of band gap limited it application in various other fields. Molybdenum Disulfide (MoS₂) has a band gap similar to Si and GaAs, which was found to very intriguing by the researchers[5]. This lead a new path to seggregate nanotechnology with semiconductor devices and opened various possibilities.

2.1.1 Structure and Properties

The properties and structure of MoS₂ changes with its dimensions. Bulk form of MoS₂ has an indirect band-gap and it is metallic in nature[9]. Whereas in the monolayer structure there is a direct band gap and its nature is semiconducting. Thickness and temperature of the flakes have a direct relation with the conductivity of the of MoS₂. According to the dimensions and bandgaps, the photoluminescence characteristics of the MoS₂ changes, which effects the optical properties. Because of the tunability of the bandgap, MoS₂ finds it application in opto-electronic devices[10]. By adding H₂O₂ as oxidizer, PL properties of MoS₂ can be enhanced without crystallinity of enhanced MoS₂.

Table 1: Comparison of Bulk and Monolayer MoS₂

Synthesis Techniques	Monolayer	Bulk
Bandgap	Indirect (1.2 eV)	Direct (1.8 eV)
Binding Energy	0.11 eV	1.1 eV
Photoluminescence Intensity	Between 10 ⁻⁵ and 10 ⁻⁶	10 ⁴ times more than that of bulk

2.1.2 Different Synthesis Techniques

There are two major type of techniques used for the synthesis of MoS₂. First being Top-down and second is bottom-up approach. Mechanical exfoliation is top-down approach and is very low cost. Only drawback is that it produces low quality flakes of MoS₂.

Physical layer deposition (PVD) and atomic layer deposition (ALD) method are two bottom-up approaches which are used to produce thin films of MoS₂. This method is low-cost and has high reproducibility[6].

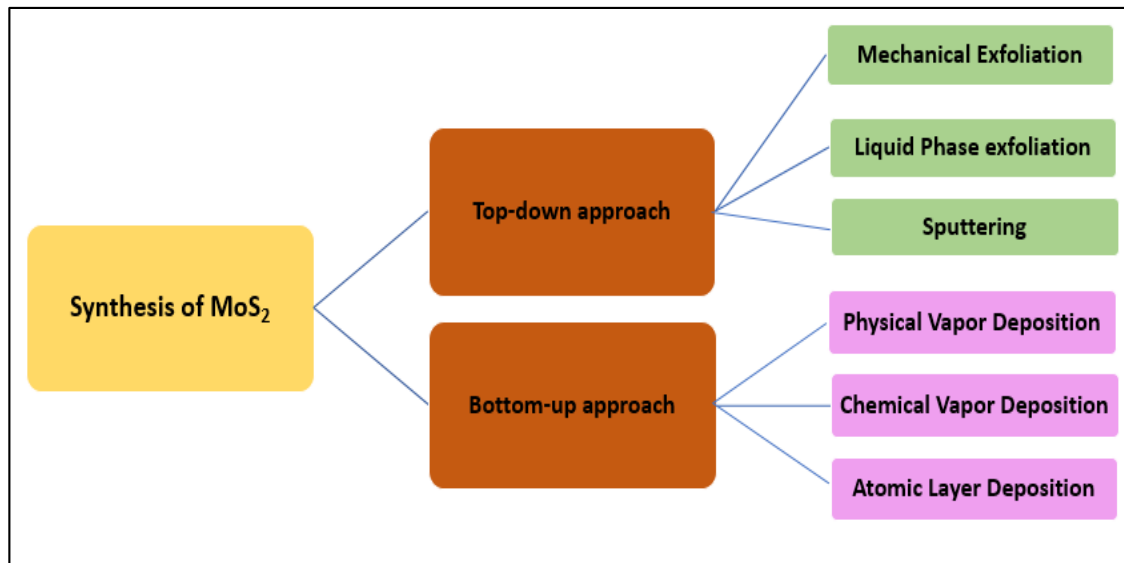


Fig. 2.1: Different MoS₂ synthesis techniques

Table 2: Summary of various synthesis techniques

Synthesis Techniques	MoS ₂ sheets Characteristics	Year	Reference
CVD with Sulfur as a precursor (Sulfidation)	on/off current ratio=10 ⁵ , mobility = 0.12 cm ² /V.s	2014	[11]
Liquid exfoliation & ultrasonic cavitation	Obtained nanosheets are in high concentration and less defective in shorter span of time.	2014	[12]
ALD & thermal evaporation	Mobility and electrical conductivity were enhanced.	2016	[13]
CVD & liquid precursor	Full coverage of substrate was ensured by water.	2017	[14]
Intercalation & exfoliation	Application found in thin-film transistors with on/off ratio of 10 ⁶ .	2018	[15]
Exfoliation of & Ultrasound Sonication in Supercritical Co ₂	Exfoliation efficiency > 90%	2019	[16]
Sulfidation	The on/off ratio of 10 ³ -10 ⁴ and electron mobility of 10-4 cm ² /V · s	2020	[17]

In , liquid precursors instead of powder precursors (MoO₂ and sulphur) were used which showed enhanced reproducibility and larger area of MoS₂. Another precursor used for synthesis of MoS₂ is sulfur vapor. In this way, molybdenum dioxide is laid on the substrate and then sulfur vapor is passed over it, to form the large area thin films[18]. CVD used with powder precursors is the best way found to synthesize the MoO₂ thin films[19]. In the table, given below summary and advancement of various synthesis techniques is mentioned.

2.2. Research Trends in 2D MoS₂ based RRAM

Liu et al.[20] was the first group to explore the potential of NVM effect in MoS₂ in which they showed RS effect in a MoS₂-PVP hybrid nanocomposite sandwiched between RGO and aluminum. Their prepared device showed RS due to detrapping and trapping of charge carriers present in MoS₂ flakes blended in organic polymer. This device exhibited a switching ratio of 10² and operating voltage of ±5 V. This paved the path for potential use of TMDCs as active material for future flexible memory applications. Later Xu et al.[21] proposed another study in which on a rigid substrate of Si, active layer of MoS₂ nanospheres was sandwiched between RGO and ITO electrodes. The device exhibited lower operating voltage (±2 V), a higher switching ratio (10⁴) and a retention time of 10⁴ s. After these successful experiments, Sun et al. showed bipolar RS behaviour in monolayer MoS₂ present between Ag and FTO (fluorine-doped tin oxide). The device showed an extremely low operating voltage (±0.4 V) and reduced power consumption because it provided electrical endurance up to 100 voltage sweeps. Bessonov et al. showed another device far superior to several other devices based on either graphene or MoS₂ in which solution-processed bilayer structure of molybdenum oxide and MoS₂ were used which exhibited a bipolar switching behavior with a very high switching ratio of 10⁶ and operating voltage (±0.2 V) shown in Fig 2.2.

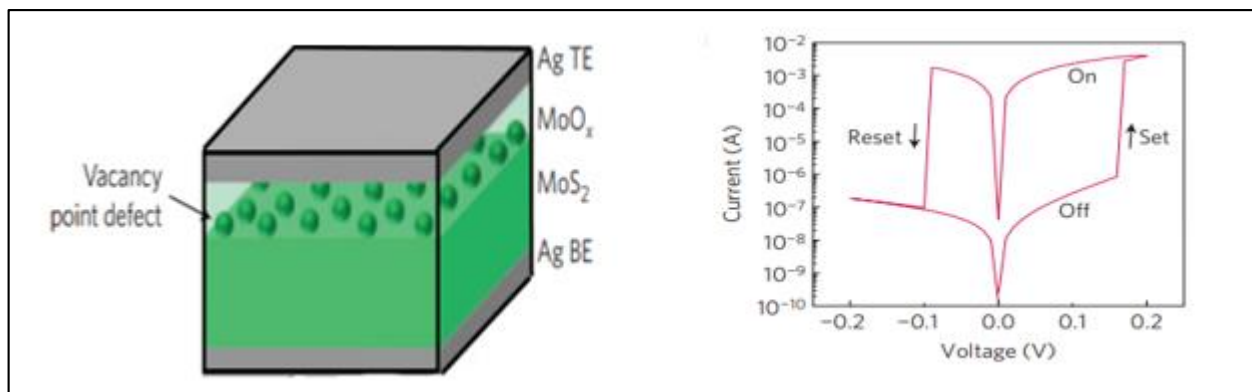


Fig. 2.2: Device structure Typical I–V curve of a MoOx/MoS₂ memristor studied by Bessonov et al.[22]

A bipolar RS in monolayer MoS₂ was reported by Sangwan et al in a field effect geometry with gate tunable characteristics of -controlled device. Sangwan et al. [7] reported the bipolar resistive switching effect in the monolayer of MoS₂ with tunable characteristics of gate-controlled device in a field effect geometry.

Monolayer of MoS₂ mediated memory phenomena in this device by the grain boundaries. By variation of voltage at gate terminal, the threshold voltage of this device was tunable from 3.5 V to 8 V. Unique aspects of MoS₂ nanosheets were explored by Cheng et al.[4] by exploring the consequences of varying MoS₂ phase on its electrical properties. They proved that the 1 T phase of exfoliated MoS₂ nano sheets sandwiched between two Ag electrodes showed a characteristic bipolar resistive switching effect and operating voltage value of ±0.2 V while the 2 H phase of bulk MoS₂ exhibited ohmic behavior.

Fan et al.[23] reported a bipolar resistive switching behavior in the Au/MoS₂-PVK/ITO (hybrid nanocomposite of MoS₂ and poly(N-vinylcarbazole)). Xia et al.[24] did a study by changing top electrode material to find that Ag was the most suitable material for the top electrode for memory

devices based on MoS₂. Redox reaction takes place inside MoS₂ thin film due to which Ag filament is formed easily. Such a device has bipolar resistive switching behavior. Ag is thus the preferred choice for the top electrode material due to its easy oxidation in MoS₂ film. Bhattacharjee et al.[8] studied the resistive memory effect in the active layer of MoS₂-PMMA nanocomposite. Kumar et al.[25] and Prakash et al.[26] reported the RS effect in MoS₂ based memory device by using Ni-Mn-In ferromagnetic shape memory alloy and tungsten nitride (W₂N) as bottom electrode instead of conventional electrode like Au, Pt, ITO, etc. Kim et al.[7] fabricated extremely low power RF switches by using the memory behavior of MoS₂ for the next generation reconfigurable communication systems and IoT. A diagrammatic representation and characterization of used materials of their proposed device is shown in fig 2.3.

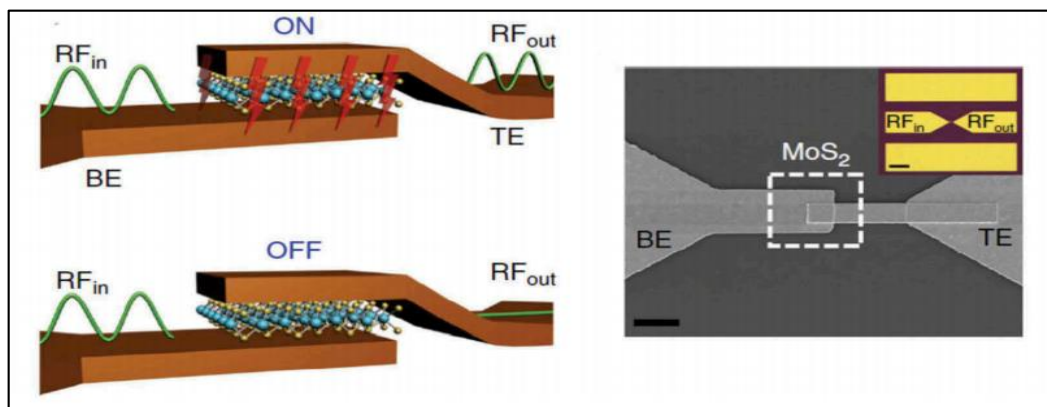


Fig. 2.3: Device structure and material characterization image. Simplified view of the device structure signal transmission of monolayer MoS₂ based RF switches.

Feng et al.[26] achieved a high switching ratio of 10⁷ in a MoS₂ based RRAM device on a flexible substrate whose diagram and optical image are shown in Figure 2.4(a). The device showed a distinctive property of both volatile and NVM behavior in a mono functional layer. Zhai et al.[27] have fabricated a MoS₂ based memory device with a distinctive feature of dual application i.e. it can be used as a memory device as well as an infrared sensor shown in fig 2.4(b). Heterostructure of MoS₂ nanosheets with upconversion nanoparticles (UCNPs) were used as the functional layer.

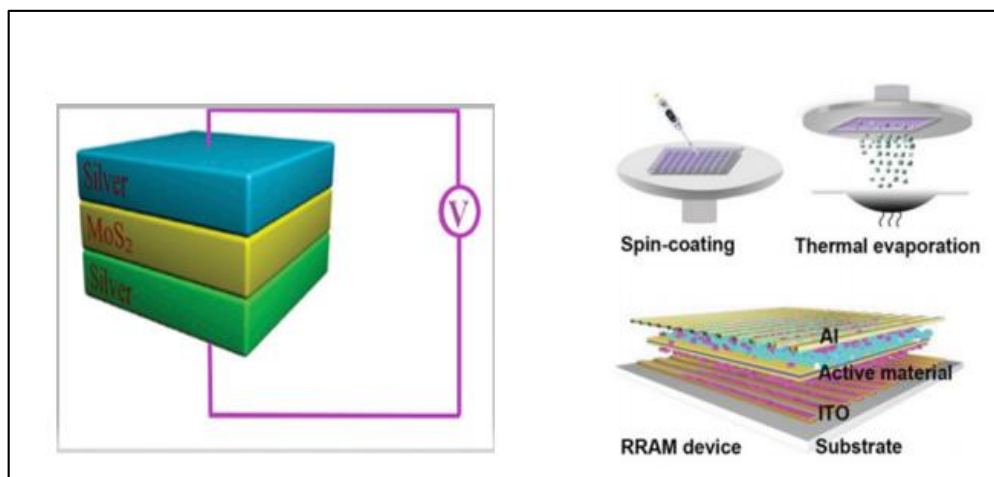


Fig. 2.4: Schematic diagram of (a) Ag/MoS₂/Ag switch and (b) Fabrication process of MoS₂-UCNPs-based RRAM device.

The summary of various MoS₂ based RRAM devices along with their typical characteristics are listed in Table 3.

Table 3: Summary of MoS₂-based RRAM device

Top electrode	Active layer	Bottom electrode	Substrate	Switching ratio	Endurance	Retention	Reference
Al	MoS ₂ -PVP	RGO	PET	10 ²	–	–	[29]
ITO	MoS ₂	RGO	SiO ₂	10 ⁴	–	10 ³	[2]
Ag	MoS ₂ /MoO _x	Ag	PEN	10 ⁶	–	10 ³	[22]
Ag	MoS ₂	FTO	Glass	10 ³	10 ²	–	[23]
Au	MoS ₂	Au	Si/SiO ₂	10 ³	–	–	[30]
Au	MoS ₂	Au	Si	10	10 ³	–	[24]
Ag	MoS ₂	Ag	Glass	–	10 ²	–	[31]
Al	MoS ₂ -PVP	ITO	PET	10 ³	10 ⁴	10 ²	[32]
Ag	MoS ₂ -PVA	Ag	PET	10 ²	10 ³	10 ⁵	[33]
Ag	MoS ₂	ITO	Glass	10 ⁴	10 ²	10 ³	[34]
Cu	MoS ₂ -PMMA	ITO	PET	10 ³	10 ⁵	10 ⁵	[35]
Au	PMMA/PMMA-MoS ₂ QDs/PMMA	FTO	Glass	10 ²	10 ²	10 ⁴	[36]
Au	MoS ₂ /PVK	ITO	–	10 ²	10 ²	10 ⁴	[33]
Al	MoS ₂ -PVK/ PEDOT:PSS	ITO	Glass	10 ²	10 ²	–	[37]
Ti/Al/Cu/Ag	MoS ₂	Ti	Si	10	–	–	[10]
Au	HfO _x /MoS ₂ /TiO _x	TiN	–	–	–	–	[38]
Al	MoS ₂	ITO	Glass	10 ²	10 ⁴	10 ⁷	[39]
Ag	MoS ₂	Ag	Kapton	10 ⁸	–	10 ⁵	[40]
Cr/Au	HfO ₂ /Al ₂ O ₃ / MoS ₂	Cr/Au	Si	10 ⁴	10 ²	10 ³	[36]
Cu	HfO ₂ /MoS ₂ MoS ₂	W ₂ N	Si	10 ³	10 ³	10 ³	[41]
Ag	ZnO/MoS ₂	Ti	Ti	2	10 ²	–	[42]
Cu	MoS ₂	Ni-Mn-In	Si	10 ²	10 ²	10 ³	[43]
Ti/Au	MoS ₂	Ti/Au	Si	–	–	–	[4]
IrO_x/Pt/Ru	Al ₂ O ₃ /TaO _x /MoS ₂	TiN	–	10 ⁵	10 ³	–	[44]
Au	MoS ₂	Au	Glass	10 ³	20	10 ⁴	[45]
ITO	HfO _x -MoS ₂ -PdNPs	ITO	Glass	10 ³	10 ²	10 ⁴	[21]
Au	MoS ₂ /PbS	Ti	Si	10 ²	10 ³	10 ⁴	[46]
Al	MoS₂-UCNPs	ITO	Glass	10⁴	10²	10⁴	[44]

CHAPTER 3

Synthesis of MoS₂ using Chemical Vapor Deposition (CVD) technique

3.1 CVD technique for synthesis of Molybdenum DiSulfide (MoS₂)

Two Dimensional layered materials such as graphene, transition metal dichalcogenides (TMDCs), hexagonal boron nitride (h-BN) have gained the attention of the scientific community due to their potential application in the field of electronic and optoelectronic device[2]. Various TMDCs that are semiconducting have been widely explored for electronic devices due to their ultrahigh mobility and semiconducting properties. Several groups have also investigated the enhanced optical properties of TMDCs in optoelectronic devices such as light-emitting diodes, phototransistors, and photovoltaics[26]. The potential use of these monolayer TMDCs is due to their high absorption coefficient and direct bandgap[47]. The application of Graphene to semiconductor devices is limited because of zero bandgap and low On/Off ratio. It acts as a semi-metal and hence no longer useful for semiconductor devices. MoS₂ emerged as an alternate choice over graphene because of the direct bandgap and high On/Off ratio. In literature, several methods have been carried out for the synthesis of the MoS₂, which include hydrothermal process, mechanical exfoliation, and chemical vapour deposition[5]. However, CVD has found to be the most practical methods to grow large-area TMDCs nanosheets. It has been most suitable for growing high-quality monolayer TMDCs[28]. In the present study, monolayer MoS₂ has been grown using the CVD technique where MoO₂ and sulfur were used as the precursor. The results reveal that the growth temperature, precursors concentration, and distance between precursors are parameters that play a pivotal role in tuning the morphology and crystalline quality of the MoS₂ nanosheet[48]. It was observed that the temperature around 750°C and the distance around 20 cm between the precursors were optimum for the monolayer growth. The grown triangular flakes have been characterized using Raman Spectroscopy and Optical microscopy. Two characteristic peaks E_{2g} and A_{1g} were observed at 381.8 cm⁻¹ and 401.5 cm⁻¹, respectively, with a distance of 19 cm⁻¹ indicating the monolayer nature. Tri-layer deposition of MoS₂ was also reported at the temperature around 750°C and the distance between the precursors was kept around 21 cm. As the difference between E¹_{2g} and A_{1g} peaks seem to increase, the monolayer is slowly moving towards the bulk nature. Optical images can also give us an idea of the layer of MoS₂ deposited on the substrate. The contrast between the substrate and the deposition increases with the number of layers[26].

3.2 Experimental Setup for Synthesis of MoS₂

MoS₂ growth on p-type <100> Si/SiO₂ substrate with oxide thickness 300 nm was carried out by using MoO₂ powder (Sigma Aldrich, 99%) and Sulfur powder (Sigma Aldrich, 99.998%) as precursors in a single zone CVD system. A diamond-tipped cutter was used to cut a 2x2 cm Si/SiO₂ substrate out of a wafer of 3-inch diameter. Substrates were first cleaned in acetone using a digital ultra-sonicator for 10 minutes. Then, the hydrophobic behaviour of the Si/SiO₂ wafer was tested under DI water, to reassure cleaning of the wafer. Argon was used as a carrier gas with a pressure of 100 sccm for the whole process.

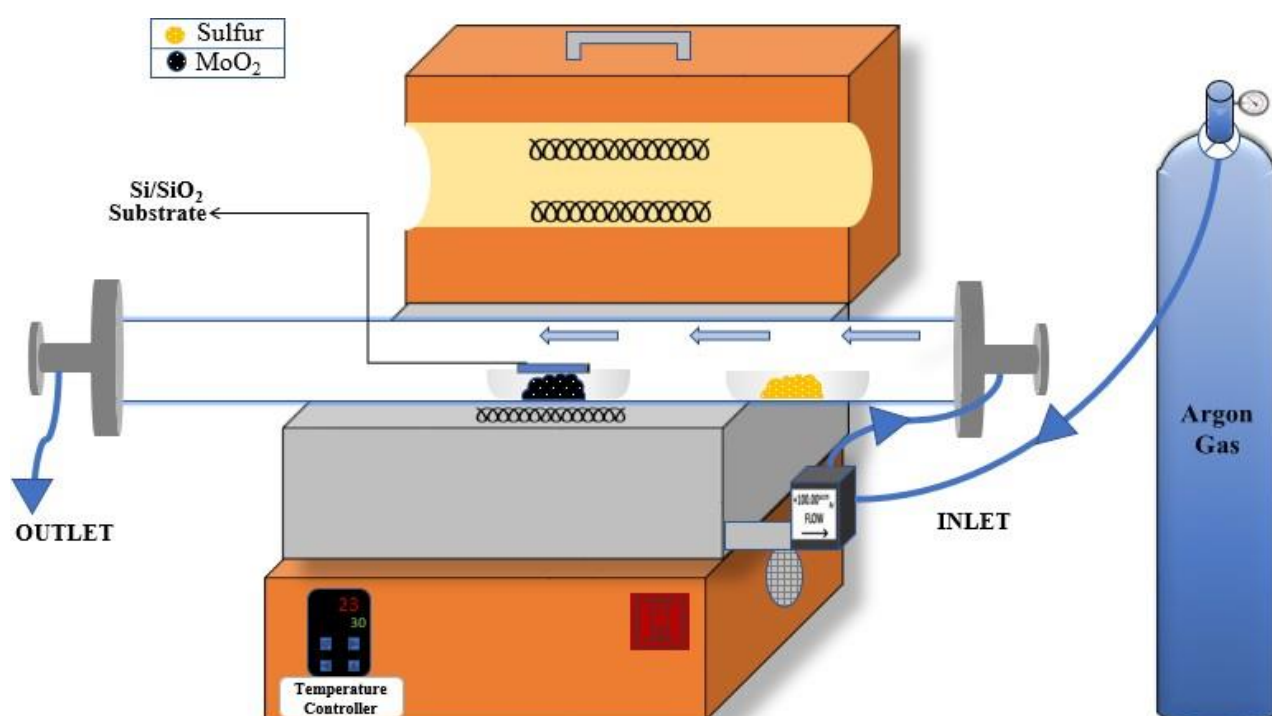


Fig. 3.1: Diagrammatic representation of Single Zone CVD Setup.

A quartz boat holding 50 mg of MoO₂ was put in the centre of the furnace at 750°C and on the same boat, Si/SiO₂ substrate was kept facing downwards. Then at a distance of 22 cm, another quartz boat holding 200 mg of Sulfur was kept. With a ramping speed of 15°C per minute, the furnace was heated and the reaction time was set for 30 minutes[9]. When the furnace started to cool down, the hood of the furnace was opened abruptly after few minutes and was then let to cool down at room temperature.

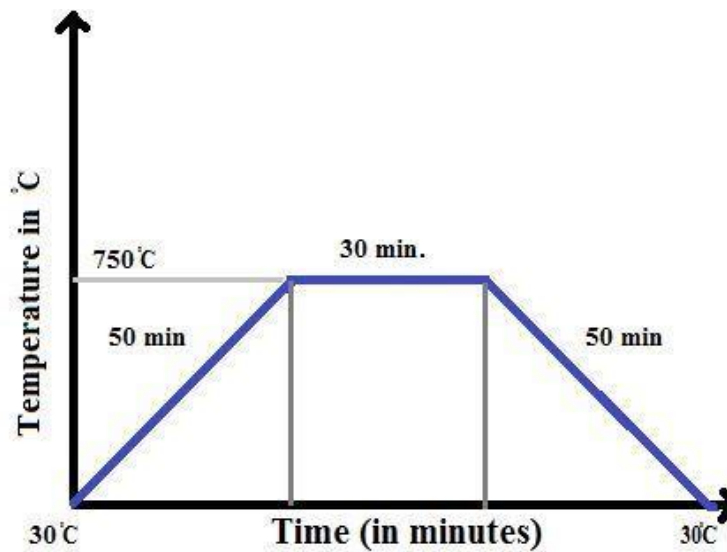


Fig. 3.2: Profile of furnace temperature vs. Time of process.

3.3 Fabrication of MoS₂ based Resistive Random-Access Memory (RRAM) Device

3.3.1 Thermal Deposition of Silver Electrodes

After the monolayer MoS₂ films were synthesized on the surface of thin-film Ag contacts were deposited. A common method of Physical vapor deposition is Thermal evaporation. The easy formation of silver filament due to the redox reaction was the reason why silver was found to be the most suitable material. 100 mg of Ag was evaporated in a vacuum environment to form a thin film on the MoS₂/Si/SiO₂ substrate. A lateral structure of the device was fabricated with Ag as positive and negative electrodes.

Deposition of Ag was carried out using thermal evaporation. Keithley source meter 2450 along with the DC probe was used for the current-voltage measurement of the fabricated device.

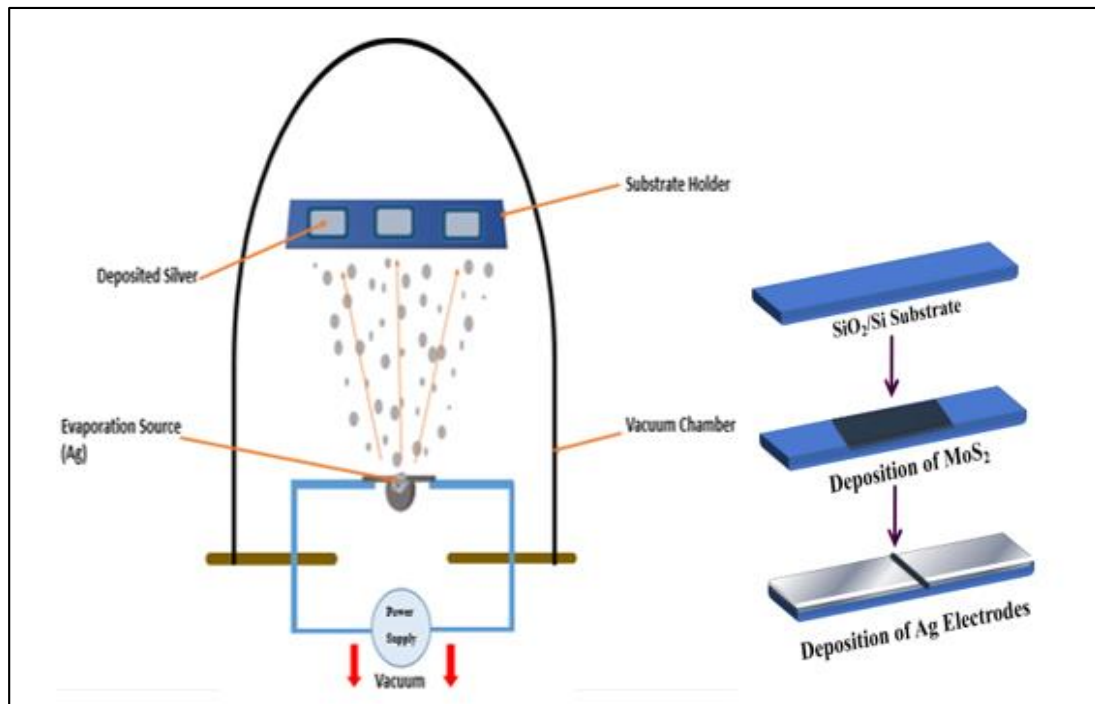


Fig. 3.3: Diagrammatic representation of thermal evaporation method.

RRAM is generally made up of two conductive electrodes with an insulating layer present in between forming a metal-insulator-metal structure. This structure can transition between a high-resistance state (HRS or logic 0) and a low-resistance state (LRS or logic 1) with the application of an appropriate voltage[8].

3.3.2 Device fabrication and electrical measurement

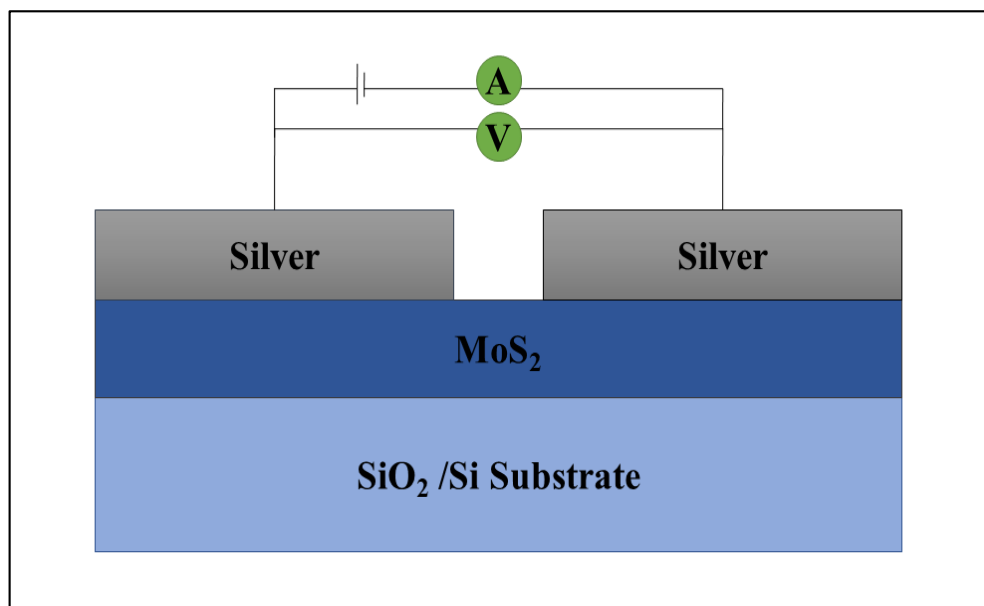


Fig.3.4: Electrical measurement and diagrammatic side view configurations of MoS₂ based memory device with Ag contacts.

Resistive random access memory (RRAM) devices show better performance compared to the traditional semiconductor electronic devices due to their resistive switching behaviour[49]. The advantage of using RRAM devices include plain device structure), multi-bit capability, lower energy consumption and its good compatibility which permits it to be combined into a current integrated circuit (IC) technology instead of the conventional CMOS. RRAM is also deployed in neuromorphic computing as a synaptic cell and low-energy consumption computing as a non-volatile logic circuit.

3.3.3 Conduction mechanism of the MoS₂ based RRAM device

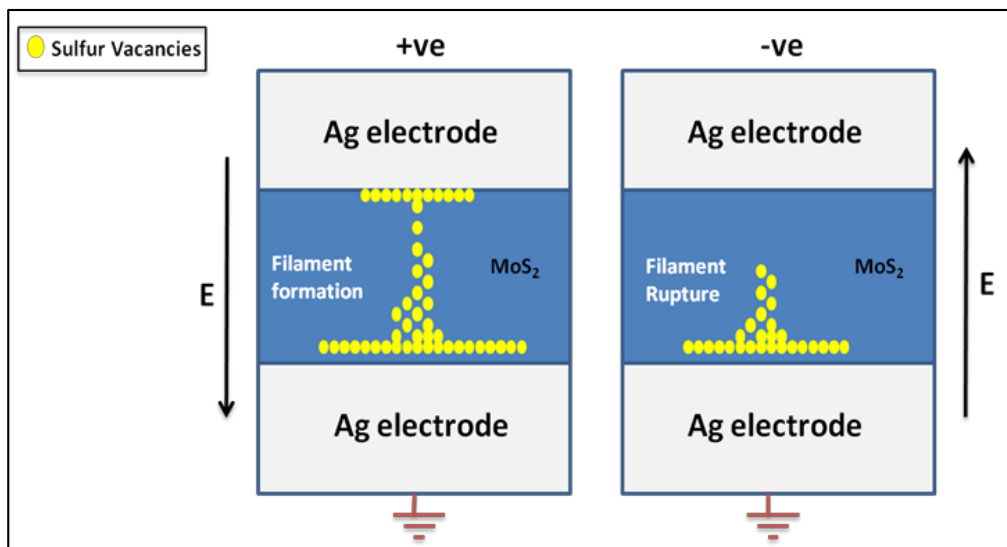


Fig. 3.5: Depicts the CF-type conduction mechanism in Ag/MoS₂/Ag device.

The sulfur vacancy is the principal defect in the MoS₂ monolayer but it does not provide a low-resistance path in its indigenous form. However, silver ions, drifting from one electrode to the other electrode can be replaced into the sulfur vacancy, which results in a conducting local density of states (LDOS), which directs it to a low resistive state. On applying a reverse electric field Ag atoms are removed, the system goes back to a high resistive state as the defects retrieve to their initial vacancy structure. At an atomic level, this switching mechanism is similar to the formation of a conductive bridge memory. The silver atoms present at the positively biased electrode become positively charged silver ions after losing their electrons ($\text{Ag} \rightarrow \text{Ag}^+ + e^-$) in the SET process. These ions are attracted by the sulfur vacancies and are simultaneously reduced ($\text{Ag}^+ + e^- \rightarrow \text{Ag}$), setting up a conductive path. The process in which the conductive filament connecting both the electrodes is formed is known as electroforming. ‘Electroforming’ or simply ‘forming’ is a necessary pre-treatment process in resistive switching. The application of either a voltage or a current leads to the development of conductive filament and consequently decreasing the cell’s resistance. Now if we apply a voltage sweep, cell’s resistance can decrease drastically at a certain voltage which causes a large increase in the power dissipation. This can destroy the cell and cause dielectric breakdown.

The resistive-switching behaviour is divided into two types unipolar and bipolar depending on voltage polarity.

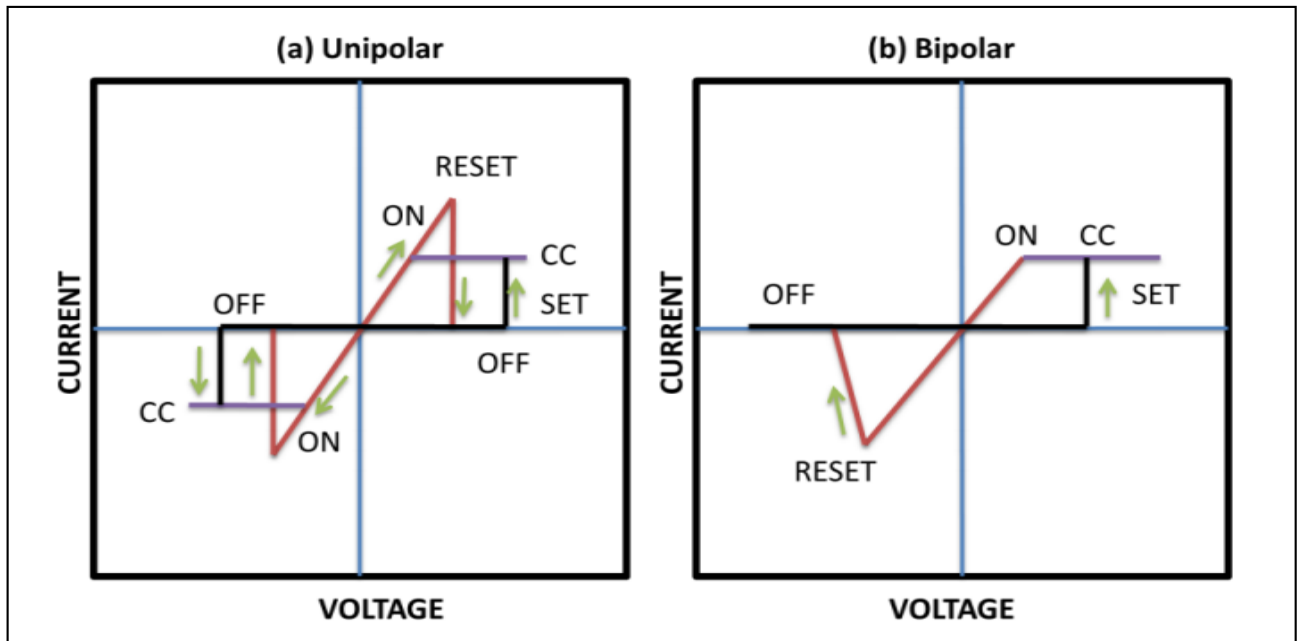


Fig.3.6. shows the current-voltage characteristics of devices with (a) unipolar switching and (b) bipolar switching.

Resistive switching is caused by a voltage having the same polarity in the case of unipolar switching, as shown in Figure 7(a) whereas in bipolar switching, shown in Figure 7(b), one polarity is employed to transition from HRS to LRS, and the opposite polarity to change back into HRS. The particular voltage at which the memory device transitions from ON to OFF state that means from low resistance state (LRS) to high resistance state (HRS) is referred to as RESET voltage while the switching OFF to ON state i.e., from HRS to LRS is referred to as the SET voltage. The resistive memory behaviour is explained by RESET and SET switching voltages. The mechanism behind the Set and Reset process is the formation and the breakage of conductive filaments which causes the resistance switching (RS) in the devices. The development and the rupture usually occur at the thinnest portion of the conducting filament owing to the electrochemical dissolution or joule heating[50].

In this study, two Ag electrodes with MoS₂ present in between define the memristor channel. Development and rupture of the conductive filament connecting the two electrodes having the monolayer MoS₂ film present in between attribute to the switching of the states.

CHAPTER 4

RESULT AND DISCUSSION

4.1 Characterization

Primary judgment about the number of layers, location, and shape of the prepared samples was made using optical microscopy(Nikon Eclipse LV100) and Raman spectroscopy. The position of characteristics Raman peaks also gives us details about whether the layer deposited is monolayer or multilayer in nature.

4.1.1 Optical Spectroscopy

Optical images of the continuous thin film of MoS₂ grown on Si/SiO₂ substrate are shown in Tables 1,2,3. On observing the optical images of the triangular flakes, a lot about the number of layers can be concluded. The growth area of the substrate is 1 cm x 1 cm, which is limited because of the small diameter of the quartz boat that was kept in CVD. On the edges of the deposited thin film, triangular flakes with edge lengths ranging from 10-45 μm were observed. Isolated triangular islands were observed of Monolayer MoS₂, whose size ranges from few microns to tens of microns.

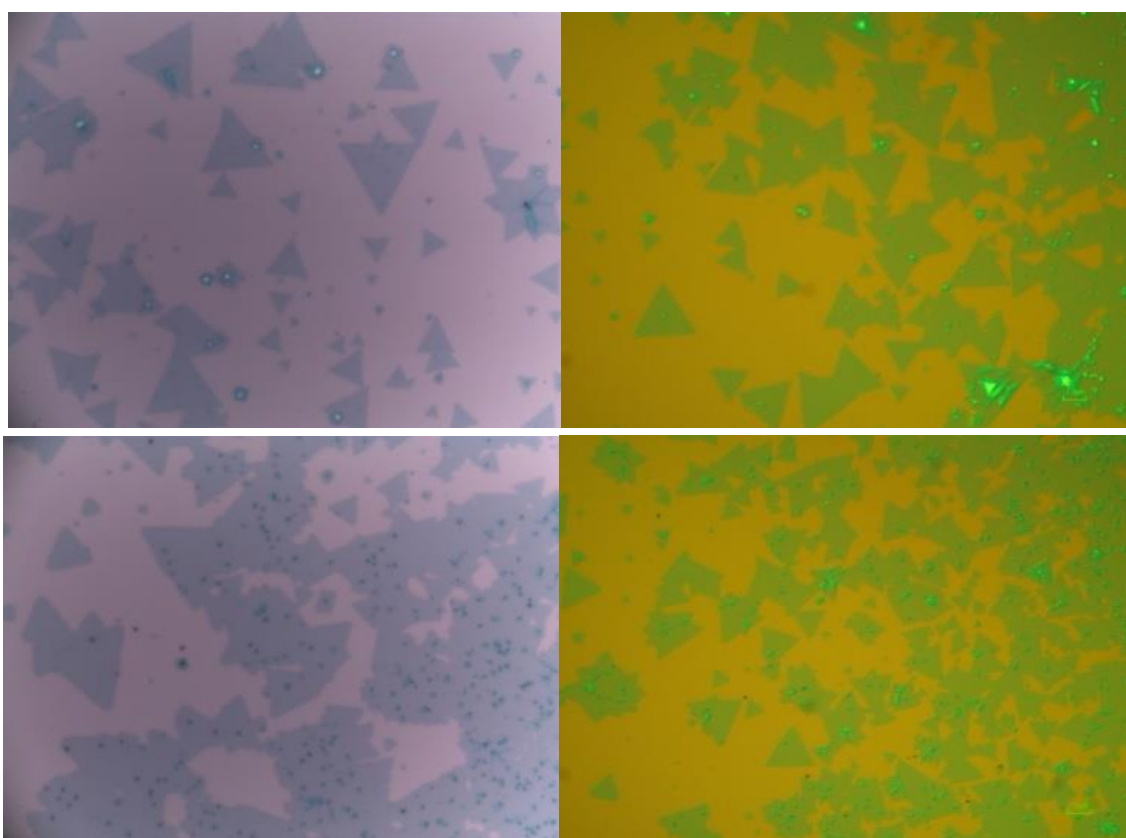


Fig. 4.1: Images showing a continuous thin film of MoS₂ grown on Si/SiO₂ substrate.

In addition to triangular islands, some other shapes like stars, and hexagons were also observed. Hexagon or merging islands are formed due to the over-deposition of MoO_2 , while star shapes are seen when the temperature of the central zone of CVD was not high enough[51]. Nucleation sites that appeared on the surface of the monolayer were resultant of the dislocation defects that occurred during the growth process. These are caused because of an excess amount of unreacted MoO_2 or excess sulfur, which created an additional site for nucleation. Owing to the longer growth/reaction time, it was found that some monolayer

MoS_2 islands were overlapping with one another[19]. This resulted in the formation of bilayer and multilayer structures[27]. Triangular flakes with edge lengths ranging from 10-45 μm were observed of the deposited thin film. An excess amount of unreacted MoO_2 or excess sulfur created an additional site on the surface of the monolayer MoS_2 for nucleation which caused the dislocation defects that occurred during the synthesis process[52]. When the thin film grown on the substrate was exposed to longer growth/reaction time, it was observed that few monolayer MoS_2 islands were overlapping with one another which resulted in the formation of bulk structures[53].

4.1.2 Raman Spectra

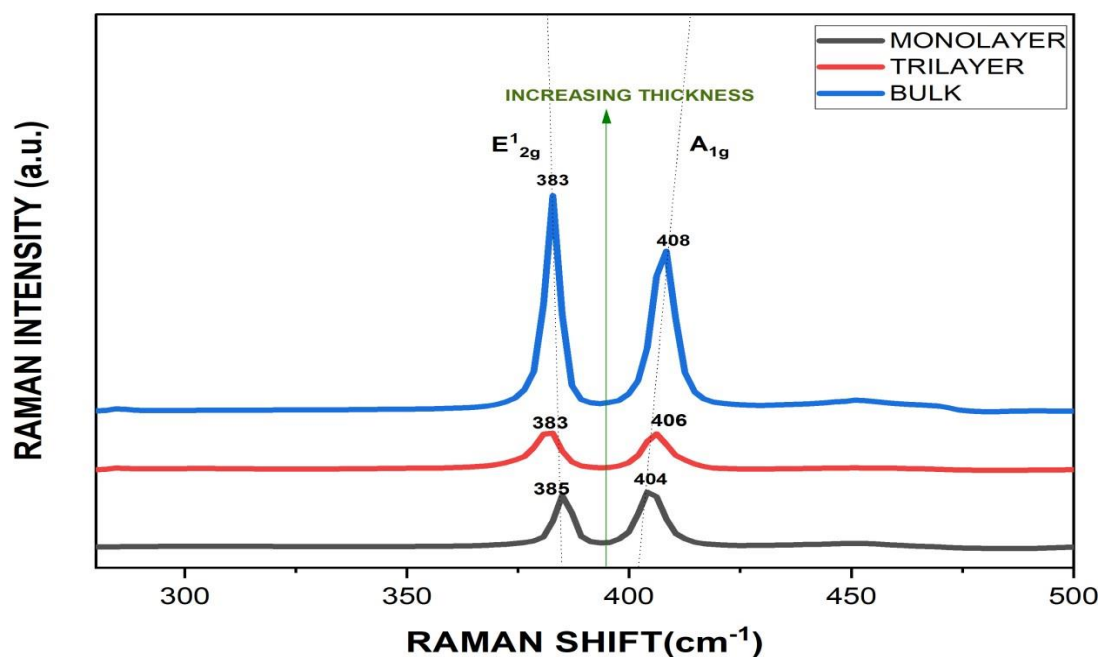


Fig. 4.2: Raman of MoS_2 thin film layer on Si/SiO_2 showing the region with the prominent E_{2g}^1 and A_{1g} peaks.

The corresponding wavenumber difference between these two characteristic peaks is 25 cm^{-1} , 23 cm^{-1} , and 19 cm^{-1} respectively. Thus, we have successfully grown large-sized, high-quality MoS_2 crystals.

Raman spectroscopy is a characterization tool that is used to study different crystalline structures of MoS₂[47]. Monochromatic laser light of wavelength 532 nm is in-elastically scattered in the visible, near-infrared, or near UV region. The laser light interacts with molecular vibrations or phonons resulting in a shift in the energy of scattered light which gives details about vibrational modes in the system. MoS₂ has two characteristic peaks known as E_{2g}¹ (in-plane mode) in which the two sulfur atoms vibrate in opposite directions to the molybdenum atoms, and A_{1g} (out-of-plane mode) in which the two sulfur atoms vibrate in opposite directions perpendicular to the plane and the frequency difference between two indicates the number of layers. When the number of layers reduces from multi-layer to monolayer the A_{1g} vibration mode undergoes a redshift while E_{2g}¹ vibration mode undergoes a blue shift. In figure 4, The bulk, tri-layer, and monolayer regions show E_{2g}¹ peaks at 383 cm⁻¹, 383 cm⁻¹, 385 cm⁻¹ and A_{1g} peak at 408 cm⁻¹, 406 cm⁻¹, 404 cm⁻¹ respectively.

4.1.3 Photoluminescence Spectroscopy (PL)

PL measurements were done to further confirm the presence of monolayer MoS₂ using a 532 nm laser (Figure 4). Strong photoluminescence in monolayer MoS₂ is seen at the direct excitonic transition energies which are not present in the indirect bandgap bulk MoS₂ films[10]. Ground state A-exciton emission is observed when a transition occurs between the conduction band and the highest valence band at the K-points[23]

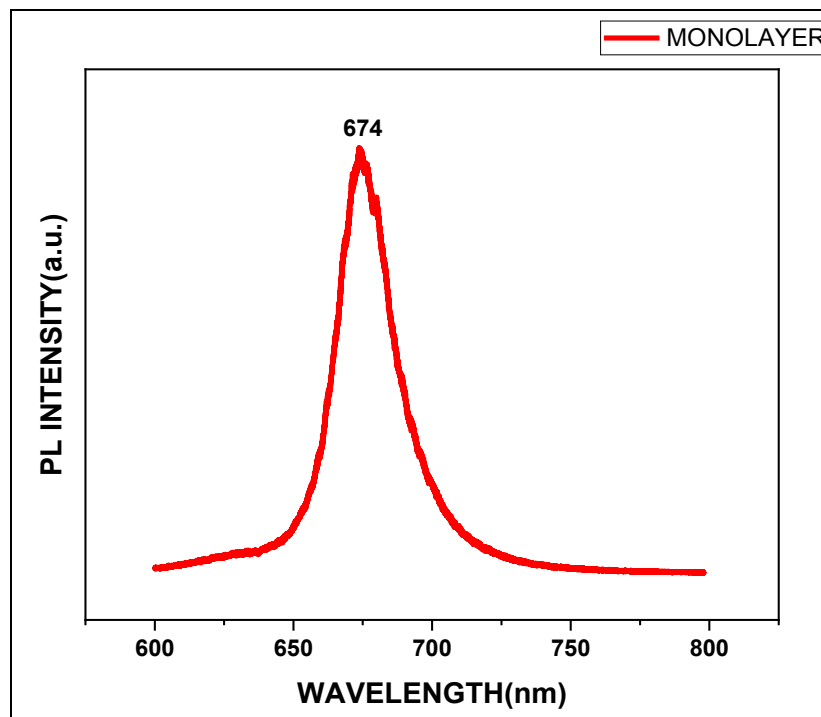


Fig. 4.3: Photoluminescence spectra of CVD-grown monolayer MoS₂.

This peak is observed at 674nm (1.84 eV) which appears because of the direct intraband recombination of the photo-generated electron-hole pairs. Thus from the PL spectra, we can conclude monolayer MoS₂ manifest a direct bandgap of 1.84eV.

4.2 Fabricated monolayer MoS₂ based RRAM Device

Thin-layer two-dimensional (2D) materials, particularly monolayer MoS₂, have unlocked new doors in the fabrication of small-scale electronic devices because of their excellent optical and electrical properties. The current techniques for the fabrication of thin layers of MoS₂ include mechanical and liquid exfoliation, physical vapor deposition, and chemical vapor deposition. Various scientific groups have followed multiple procedures for the good crystalline growth of monolayer MoS₂. The chemical vapor deposition (CVD) technique is the most victorious and authentic method for large-scale and thickness-dependent growth among all the other known methods. The growth conditions, shape and size of MoS₂ flakes are considerably dominated by factors including pressure, growth temperature, growth time, the concentration of precursors, etc. Molybdenum Disulfide (MoS₂) is an n-type semiconductor that has emerged as the most suitable contender in electronic devices. Monolayer MoS₂ which is diamagnetic undergoes a transition to direct bandgap from indirect bandgap when the layer number decreases from the bulk form to monolayer. As the number of layers increases, the bandgap decreases. Various approaches to fabricate MoS₂ include liquid intercalation, hydrothermal method, mechanical exfoliation, and chemical vapor deposition (CVD). In this study, we have overcome the challenge of synthesizing high-quality monolayer films of MoS₂. The growth of monolayer MoS₂ films was successfully done by optimizing various parameters like concentration, reaction time, reaction temperature, pressure, and placements of boats. Field-effect transistors (FETs) based on monolayer MoS₂ have pre-eminent importance in future electronic applications such as data storage, memory, optoelectronics, quantum optics, communication, etc. because of their high ON/OFF current ratios, their high electron-hole mobility, low operation power, and good photo-responsivity. In this study, the CVD technique was used wherein MoO₂ powder and sulphur powder were used as reactants. Raman spectroscopy and photoluminescence (PL) spectroscopy were carried out to assess the optical as well as structural properties of the grown MoS₂ thin films. The Raman characteristic peaks 384cm⁻¹ (E_{2g}) and 404cm⁻¹ (A_{1g}) manifest that the grown film is monolayer MoS₂. A pronounced emission peak was observed at 674 nm in the photoluminescence spectrum of monolayer MoS₂. The results revealed that we have grown monolayer MoS₂ with an optical bandgap of 1.84eV.

RRAM is a two-terminal structure that is operated by applying a sufficiently high voltage which changes the resistance state to store information in a non-volatile manner.

We have studied MoS₂ based devices for memory applications particularly for fabrication of RRAM, and have obtained the desired result for electric switching between the semiconductor phase to the metallic phase. The device was fabricated using thermal evaporation of silver onto the thin films of MoS₂ on SiO₂/Si substrate. In literature, various electrodes like tin, copper, silver, and aluminium were used for MoS₂ based memory devices. The redox reaction that takes place inside MoS₂ thin films due to the easy formation of silver filament is the reason why silver is found to be the most suitable material for the fabrication of memory device. Monolayer MoS₂ based memory devices show faster switching due to the high On/off ratio. The RRAM device show promising features because of their probable scalability, high endurance, high operation speed, and process flow ease in comparison to the flash memories.

4.3 Experimental Results

4.3.1 Effect of Variation of parameters on the growth of MoS₂

Table 4: Effect of Concentration of Precursors.

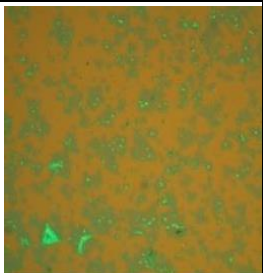
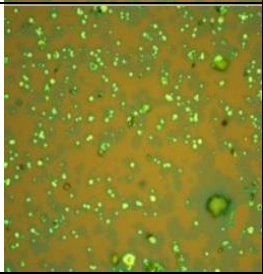
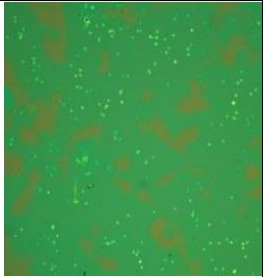
S.No	MoO ₂ (Weight in mg)	Sulfur (Weight in mg)	Distance b/w boats (in cm)	Temperature of the centre zone (in °C)	Reaction time (in minutes)	Inference	Optical Images
1.	40	160	20	750	20	Bi-layer (triangle)	
2.	20	160	20	750	20	Excess Sulfur	
3.	60	240	20	750	20	Bulk (Merging islands)	

Table 5: Effect of Distance between Boats containing Precursors

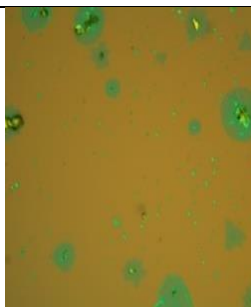
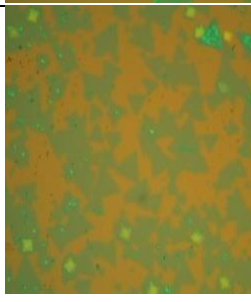
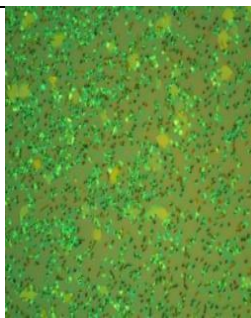
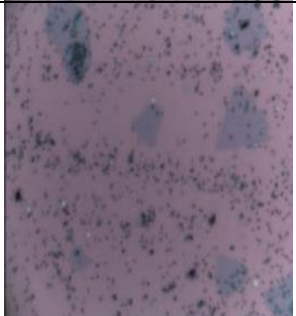

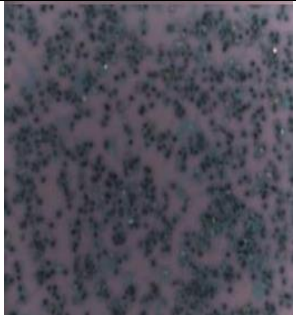
S.No.	MoO ₂ (Weight in mg)	Sulfur (Weight in mg)	Distance b/w boats (in cm)	Temperature of the centre zone (in ° C)	Reaction time (in minutes)	Inference	Optical Images
1.	50	200	22	750	20	Bulk (Merging Islands)	
2.	50	200	21	750	20	Tri-Layer.	
3.	50	200	19	750	20	Bulk (Unreacted MoO ₂)	

Table 6: Effect of Temperature of the central zone of CVD

S.No	MoO ₂ (Weight in mg)	Sulfur (Weigt in mg)	Distance b/w boats (in cm)	Temperature of the center zone (in °C)	Reaction time (in minute)	Inference	Optical Images
1.	50	200	20	720	20	Bulk	
2.	50	200	20	750	20	Monolayer (triangle)	
3.	50	200	20	780	20	Bulk	

4.4 Transfer characteristics of prepared RRAM (Ag/MoS₂/Ag) Device

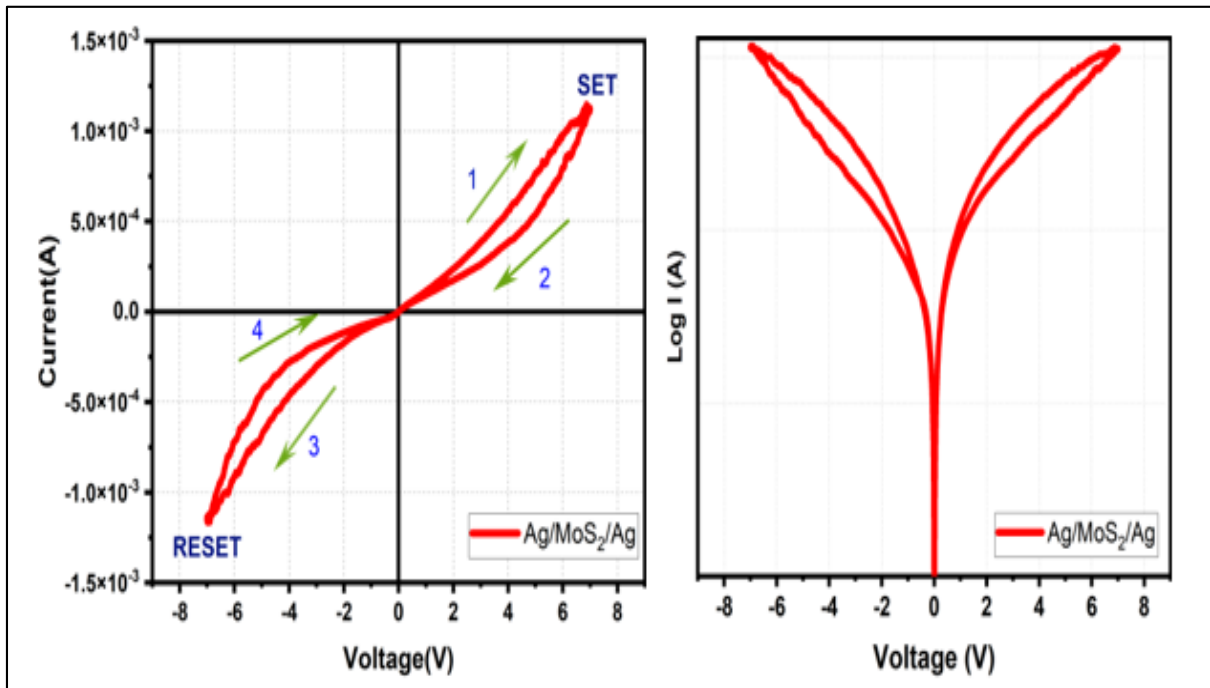


Fig. 4.4: (a) linear plot and (b) semi-logarithmic plot for the same two-probe transfer characteristics for a typical Ag/MoS₂/Ag device. The voltage was swept in the sequence of 0 V → 7V → 0 V → -7 V → 0 V, as shown by the coloured arrows with the four sweeps labelled as 1, 2, 3 and 4.

Dielectric breakdown causes an indefinite decrease in the cell's resistance which makes the transition back to the HRS not possible. To avoid such a situation a current compliance function is provided that can manage the maximum current (known as compliance current) flowing in the cell. D.C. electrical measurements were performed on the prepared Ag/MoS₂/Ag device configuration by sweeping the tip bias. It is observed that the device manifest bipolar switching with On/Off ratio of 10³.

CHAPTER 5

Conclusion and Future Scope

5.1 Conclusion

In the present work, the effect of various parameters in the synthesis of the MoS₂ films on Si/SiO₂ substrate by single-zone chemical vapor deposition technique using MoO₃ and sulfur as precursors is studied. The MoS₂ films synthesized were monolayer, tri-layer, and bulk in nature, as reported by Raman Spectroscopy and Optical Microscopy. The presence of monolayer film was attested by optical microscopy, Raman spectroscopy, and Photoluminescence Spectroscopy. It may be highlighted that the role of concentration of precursors, the temperature of the furnace, and distance between boats carrying precursors were found to be pivotal in the desired growth of the monolayer MoS₂.

Further we have explained the resistive switching mechanism in Ag/MoS₂/Ag memory device. The formation/rupture of conductive filament has been demonstrated elaborately for the prepared device. The fabricated Ag/MoS₂/Ag memory device exhibits a bipolar resistive switching phenomenon. This study opens more doors for RRAM devices in future non-volatile memory applications.

After Graphene, MoS₂ is one of the most widely explored TMDs for the fabrication of non-volatile RRAMs. Other 2D materials such as WS₂, MoSe₂, WSe₂ and hBN are also explored as the active layer of future NVMs.

Based on the procured results, the following conclusions can be deduced:

- a) The results revealed that the growth temperature, precursors concentration, and distance between precursors are parameters that play a pivotal role in tuning the morphology and crystalline quality of the MoS₂ nanosheets.
- b) It was observed that the temperature around 750°C and the distance around 20 cm between the precursors were optimum for the monolayer growth.
- c) As the difference between E_{2g} and A_{1g} peaks seem to increase, the monolayer is slowly moving towards the bulk nature.
- d) Even when the same active layer of MoS₂ is used, the memory characteristics are different from each other. That implies that there must be some other factors that are controlling the characteristics of the RRAM devices i.e. thickness of the deposited thin film, electrode's element etc.
- e) Desired results for electric switching between the semiconductor phase to the metallic phase were obtained.
- f) The redox reaction that takes place inside MoS₂ thin films due to the easy formation of silver filament is the reason why silver is found to be the most suitable material for fabrication of memory device.
- g) Monolayer MoS₂ based memory devices show faster switching due to the high On/off ratio.

5.2 Future Scope

Within only a decade of research on 2D-materials based RRAMs, they have shown a promising future with a comparatively low voltages of operation and better switching speeds. On the basis of previous research on 2D-materials based RRAMs, following conclusions can be drawn :

- a) One of the key areas in the development of 2D materials based RRAMs is the various fabrication techniques. There are various techniques of the fabrication being developed for RRAMS, but none of them is found to be effective in manufacturing devices on larger scale and industrial level.
- b) Second area where there is scope of development is to make the fabrication process of these layers of 2D-materials to be transfer-free. The transfer-free fabrication will lead to a crack-free surface which in turn will increase the device characteristics and switching mechanisms.
- c) Better device designs and structures can be opted for finer device performance. Different designs of fabrication, materials and layers have been varied to better the performance of the RRAMs devices based on the 2D-materials.
- d) Another significant area open for further research is to explore the switching mechanism and resistive behaviour. This can be done choosing different material for electrodes and by varying the thickness of the thin-films.
- e) Lack of efficient characterization technique for the nanosurfaces is another area for development in the field of development of 2D-materials based RRAMs.
- f) A pocket friendly development system can be made if simulation softwares like COMSOL is used to design the devices by varying parameters like film thickness, structure of device to monitor its effect on resistive behaviour and conduction mechanism.

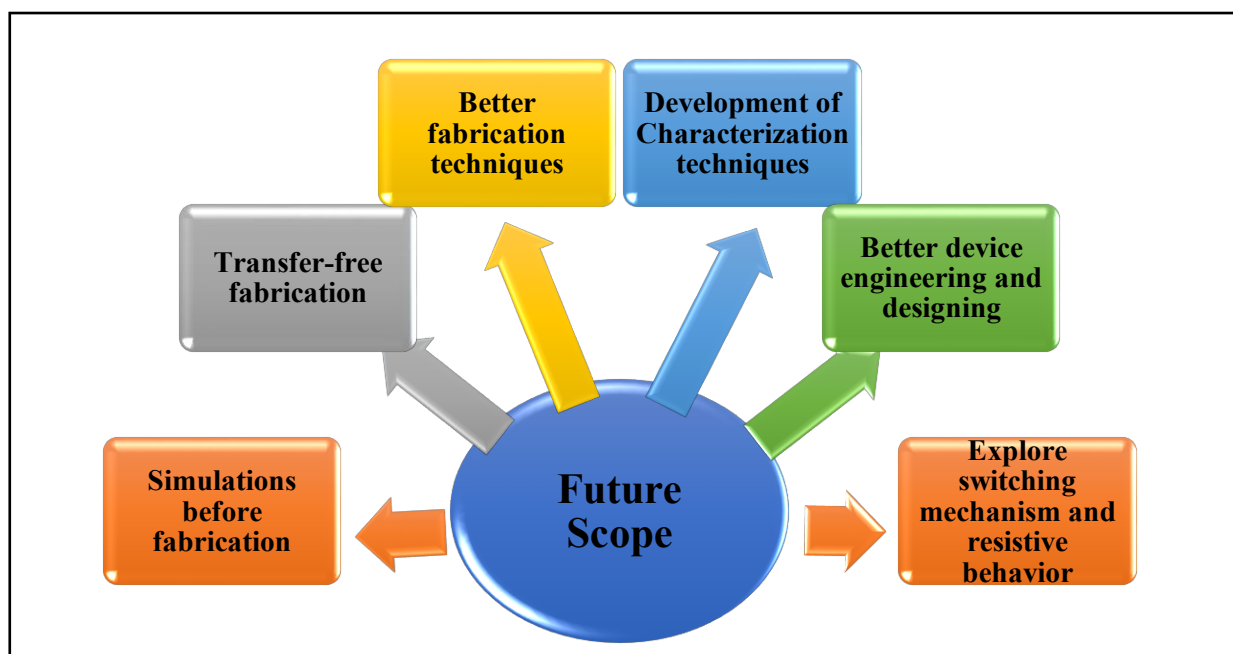


Fig. 5.1: Future prospect of 2D-materials based RRAM devices.

REFERENCES

- [1] A. Manuscript, "Nanoscale," 2017, doi: 10.1039/C7NR01755C.
- [2] R. Xu *et al.*, "Vertical MoS₂ Double-Layer Memristor with Electrochemical Metallization as an Atomic-Scale Synapse with Switching Thresholds Approaching 100 mV," *Nano Lett.*, vol. 19, no. 4, pp. 2411–2417, 2019, doi: 10.1021/acs.nanolett.8b05140.
- [3] M. Imran, N. Chaudhary, A. K. Hafiz, B. Singh, and M. Khanuja, "CVD synthesis and characterization of ultrathin MoS₂ film," *AIP Conf. Proc.*, vol. 2276, no. October, 2020, doi: 10.1063/5.0026128.
- [4] Y. H. Lee *et al.*, "Synthesis of large-area MoS₂ atomic layers with chemical vapor deposition," *Adv. Mater.*, vol. 24, no. 17, pp. 2320–2325, 2012, doi: 10.1002/adma.201104798.
- [5] A. Splendiani *et al.*, "Emerging photoluminescence in monolayer MoS₂," *Nano Lett.*, vol. 10, no. 4, pp. 1271–1275, 2010, doi: 10.1021/nl903868w.
- [6] J. C. Scott and L. D. Bozano, "Nonvolatile memory elements based on organic materials," *Adv. Mater.*, vol. 19, no. 11, pp. 1452–1463, 2007, doi: 10.1002/adma.200602564.
- [7] M. M. Rehman *et al.*, "Decade of 2D-materials-based RRAM devices : a review Decade of 2D-materials-based RRAM devices : a review," *Sci. Technol. Adv. Mater.*, vol. 21, no. 1, pp. 147–186, 2020, doi: 10.1080/14686996.2020.1730236.
- [8] S. Yu, R. Jeyasingh, Y. Wu, and H. S. Philip Wong, "Understanding the conduction and switching mechanism of metal oxide RRAM through low frequency noise and AC conductance measurement and analysis," *Tech. Dig. - Int. Electron Devices Meet. IEDM*, pp. 275–278, 2011, doi: 10.1109/IEDM.2011.6131537.
- [9] X. Zhao *et al.*, "Reversible alternation between bipolar and unipolar resistive switching in Ag/MoS₂/Au structure for multilevel flexible memory," *J. Mater. Chem. C*, vol. 6, no. 27, pp. 7195–7200, 2018, doi: 10.1039/c8tc01844h.
- [10] T. Han *et al.*, "Research on the factors affecting the growth of large-size monolayer MoS₂ by APCVD," *Materials (Basel)*, vol. 11, no. 12, 2018, doi: 10.3390/ma11122562.
- [11] Y. Lee *et al.*, "Synthesis of wafer-scale uniform molybdenum disulfide films with control over the layer number using a gas phase sulfur precursor," *Nanoscale*, vol. 6, no. 5, pp. 2821–2826, 2014, doi: 10.1039/c3nr05993f.
- [12] J. T. Han *et al.*, "Extremely efficient liquid exfoliation and dispersion of layered materials by unusual acoustic cavitation," *Sci. Rep.*, vol. 4, pp. 1–7, 2014, doi: 10.1038/srep05133.
- [13] S. J. Kim *et al.*, "Large-scale Growth and Simultaneous Doping of Molybdenum Disulfide Nanosheets," *Sci. Rep.*, vol. 6, no. October 2015, pp. 1–7, 2016, doi: 10.1038/srep24054.
- [14] S. H. Choi *et al.*, "Water-Assisted Synthesis of Molybdenum Disulfide Film with Single Organic Liquid Precursor," *Sci. Rep.*, vol. 7, no. 1, pp. 1–8, 2017, doi: 10.1038/s41598-017-02228-8.
- [15] Z. Lin *et al.*, "Solution-processable 2D semiconductors for high-performance large-area electronics," *Nature*, vol. 562, no. 7726, pp. 254–258, 2018, doi: 10.1038/s41586-018-0574-4.

- [16] X. Tan, W. Kang, J. Liu, and C. Zhang, "Synergistic Exfoliation of MoS₂ by Ultrasound Sonication in a Supercritical Fluid Based Complex Solvent," *Nanoscale Res. Lett.*, vol. 14, no. 1, 2019, doi: 10.1186/s11671-019-3126-4.
- [17] H. Kim *et al.*, "Sulfidation characteristics of amorphous nonstoichiometric Mo-oxides for MoS₂ synthesis," *Appl. Surf. Sci.*, vol. 535, no. April 2020, p. 147684, 2021, doi: 10.1016/j.apsusc.2020.147684.
- [18] O. Samy, S. Zeng, M. D. Birowosuto, and A. El Moutaouakil, "A Review on MoS₂ Properties, Synthesis, Sensing Applications and Challenges," pp. 1–24, 2021.
- [19] D. Zhu, H. Shu, F. Jiang, D. Lv, V. Asokan, and O. Omar, "Capture the growth kinetics of CVD growth of two-dimensional MoS₂," pp. 1–24.
- [20] D. Ma *et al.*, "A universal etching-free transfer of MoS₂ films for applications in photodetectors," 2015, doi: 10.1007/s12274-015-0866-z.
- [21] X. Wang, H. Tian, H. Zhao, T. Zhang, and W. Mao, "Interface Engineering with MoS₂ – Pd Nanoparticles Hybrid Structure for a Low Voltage Resistive Switching Memory," vol. 1702525, pp. 1–8, 2017, doi: 10.1002/sml.201702525.
- [22] A. A. Bessonov, M. N. Kirikova, D. I. Petukhov, M. Allen, T. Ryhänen, and M. J. A. Bailey, "Layered memristive and memcapacitive switches for printable electronics," no. November, 2014, doi: 10.1038/NMAT4135.
- [23] L. Sun *et al.*, "Vacuum level dependent photoluminescence in chemical vapor deposition-grown monolayer MoS₂," *Sci. Rep.*, vol. 7, no. 1, pp. 1–9, 2017, doi: 10.1038/s41598-017-15577-1.
- [24] W. Wang, G. N. Panin, X. Fu, L. Zhang, and P. Ilanchezhian, "MoS₂ memristor with photoresistive switching," no. July, pp. 1–10, 2016, doi: 10.1038/srep31224.
- [25] L. P. L. Mawlong, K. K. Paul, and P. K. Giri, "Direct Chemical Vapor Deposition Growth of Monolayer MoS₂ on TiO₂ Nanorods and Evidence for Doping-Induced Strong Photoluminescence Enhancement," *J. Phys. Chem. C*, vol. 122, pp. 15017–15025, 2018, doi: 10.1021/acs.jpcc.8b03957.
- [26] N. R. Pradhan *et al.*, "CVD-grown monolayered MoS₂ as an effective photosensor operating at low-voltage counter electrodes CVD-grown monolayered MoS₂ as an effective photosensor operating at low-voltage," 2014, doi: 10.1088/2053-1583/1/1/011004.
- [27] J. Chen *et al.*, "Chemical Vapor Deposition of High-Quality Large-Sized MoS₂ Crystals on Silicon Dioxide Substrates," no. March, 2016, doi: 10.1002/advs.201600033.
- [28] F. Zahoor, T. Z. Azni Zulkifli, and F. A. Khanday, "Resistive Random Access Memory (RRAM): an Overview of Materials, Switching Mechanism, Performance, Multilevel Cell (mlc) Storage, Modeling, and Applications," *Nanoscale Res. Lett.*, vol. 15, no. 1, 2020, doi: 10.1186/s11671-020-03299-9.
- [29] J. Liu, Z. Zeng, X. Cao, G. Lu, L. Wang, and Q. Fan, "Preparation of MoS₂-Polyvinylpyrrolidone Nanocomposites for Flexible Nonvolatile Rewritable Memory Devices with Reduced Graphene Oxide Electrodes," pp. 1–6, 2012, doi: 10.1002/sml.201200999.
- [30] V. K. Sangwan *et al.*, "Gate-tunable memristive phenomena mediated by grain boundaries in single-layer MoS₂," *Nat. Nanotechnol.*, vol. 10, no. 5, pp. 403–406, 2015, doi: 10.1038/nnano.2015.56.

- [31] P. Cheng, K. Sun, and Y. H. Hu, "Memristive Behavior and Ideal Memristor of 1T Phase MoS₂ Nanosheets," 2015, doi: 10.1021/acs.nanolett.5b04260.
- [32] P. Yang *et al.*, "Batch production of 6-inch uniform monolayer molybdenum disulfide catalyzed by sodium in glass," *Nat. Commun.*, no. 2018, pp. 1–10, doi: 10.1038/s41467-018-03388-5.
- [33] M. M. Rehman, G. U. Siddiqui, J. Z. Gul, and S. Kim, "Resistive Switching in All-Printed, Flexible and Hybrid MoS₂-PVA Nanocomposite based Memristive Device Fabricated by Reverse Offset," *Nat. Publ. Gr.*, no. June, pp. 1–10, 2016, doi: 10.1038/srep36195.
- [34] Y. Xia *et al.*, "Metal ion formed conductive filaments by redox process induced nonvolatile resistive switching memories in MoS₂ film," *Appl. Surf. Sci.*, 2017, doi: 10.1016/j.apsusc.2017.07.257.
- [35] H. Search *et al.*, "ce pte d M us pt," 2017.
- [36] D. Wang, F. Ji, X. Chen, Y. Li, B. Ding, and Y. Zhang, "device Quantum conductance in MoS₂ quantum dots-based nonvolatile resistive memory device," vol. 093501, 2017, doi: 10.1063/1.4977488.
- [37] L. Guan *et al.*, "Thiol-modified MoS₂ nanosheets as a functional layer for electrical bistable devices," no. April, 2017, doi: 10.1016/j.optcom.2017.07.035.
- [38] P. Chen *et al.*, "An RRAM with a 2D Material Embedded Double Switching Layer for Neuromorphic Computing," *2018 IEEE 13th Nanotechnol. Mater. Devices Conf.*, vol. 1, pp. 1–4, 2018, doi: 10.1109/NMDC.2018.8605915.
- [39] X. Liang, "MoS₂ Memristors Exhibiting Variable Switching Characteristics towards Bio-Realistic Synaptic Emulation," 2018, doi: 10.1021/acsnano.8b03977.
- [40] X. Feng *et al.*, "T8-4 First Demonstration of a Fully-Printed MoS₂ RRAM on Flexible Substrate with Ultra-Low Switching Voltage and its Application as Electronic Synapse T88 T89," *2019 Symp. VLSI Technol.*, pp. T88–T89, 2019.
- [41] M. Graf *et al.*, *Fabrication and practical applications of molybdenum disulfide nanopores*. Springer US.
- [42] M. S. Kadhim *et al.*, "Existence of Resistive Switching Memory and Negative Differential Resistance State in Self-Colored MoS₂/ZnO Heterojunction Devices," *ACS Appl. Electron. Mater.*, vol. 1, pp. 318–324, 2019, doi: 10.1021/acsaelm.8b00070.
- [43] A. Kumar, S. Pawar, S. Sharma, and D. Kaur, "Bipolar resistive switching behavior in MoS₂ nanosheets fabricated on ferromagnetic shape memory alloy," vol. 262106, 2018, doi: 10.1063/1.5037139.
- [44] M. U. Heterostructure *et al.*, "Infrared-Sensitive Memory Based on Direct-Grown," vol. 1803563, pp. 1–9, 2018, doi: 10.1002/adma.201803563.
- [45] M. Kim *et al.*, "Zero-static power radio-frequency switches based on MoS₂ atomristors," *Nat. Commun.*, no. 2018, pp. 1–7, doi: 10.1038/s41467-018-04934-x.

- [46] Q. Wang *et al.*, “Nonvolatile infrared memory in MoS₂ / PbS van der Waals heterostructures,” no. April, pp. 1–8, 2018.
- [47] B. Birmingham *et al.*, “Spatially-Resolved Photoluminescence of Monolayer MoS₂ under Controlled Environment for Ambient Optoelectronic Applications,” *ACS Appl. Nano Mater.*, vol. 1, no. 11, pp. 6226–6235, 2018, doi: 10.1021/acsanm.8b01422.
- [48] H. Van Ngoc, Y. Qian, S. K. Han, and D. J. Kang, “PMMA-Etching-Free Transfer of Wafer-scale Chemical Vapor Deposition Two-dimensional Atomic Crystal by a Water Soluble Polyvinyl Alcohol Polymer Method,” *Nat. Publ. Gr.*, no. August, pp. 1–9, 2016, doi: 10.1038/srep33096.
- [49] R. Yang *et al.*, “2D Molybdenum Disulfide (MoS₂) Transistors Driving RRAMs with 1T1R Configuration,” pp. 477–480, 2017, doi: 10.1021/acsnano.7b04100.
- [50] J. Wang *et al.*, “Magnetic field controllable nonvolatile resistive switching effect in silicon device,” *Appl. Phys. Lett.*, vol. 104, no. 24, 2014, doi: 10.1063/1.4884771.
- [51] Maiti and Bidinger, “~~濟無~~No Title No Title,” *J. Chem. Inf. Model.*, vol. 53, no. 9, pp. 1689–1699, 1981.
- [52] P. Shen and M. S. Photonics, “Large-area CVD Growth of Two-dimensional Transition Metal Dichalcogenides and Monolayer MoS₂ and WS₂ Metal – oxide – semiconductor Field-effect Transistors by Master of Science in Electrical Engineering,” pp. 1–55, 2017.
- [53] R. Lewandowska, H. Scientific, D. Lille, and V. Ascq, “Number of layers of MoS₂ determined using Raman Spectroscopy,” pp. 54–55.
- [54] D. Falola and I. Suni, “Electrodeposition of MoS₂ for Charge Storage in Electrochemical Supercapacitors,” vol. 9, no. 9, 2016, doi: 10.1149/2.0011610jes.This.
- [55] Z. D. Ganger, “Growth of Two-Dimensional Molybdenum Disulfide via Chemical Vapor Deposition GROWTH OF TWO-DIMENSIONAL MOLYBDENUM,” 2019.
- [56] K. Thakar and S. Lodha, “Optoelectronic and photonic devices based on transition metal dichalcogenides,” *Mater. Res. Express*, vol. 7, no. 1, 2019, doi: 10.1088/2053-1591/ab5c9c.
- [57] Z. Shen, C. Zhao, Y. Qi, I. Z. Mitrovic, and L. Yang, “Memristive Non-Volatile Memory Based on Graphene Materials.”
- [58] E. Rotunno, M. Bosi, L. Seravalli, G. Salviati, and F. Fabbri, “Influence of organic promoter gradient on the MoS₂ growth dynamics,” *Nanoscale Adv.*, vol. 2, no. 6, pp. 2352–2362, 2020, doi: 10.1039/d0na00147c.
- [59] H. Zhang, “Nucleation and Growth Mechanisms of 2D Semiconductor / high- ϵ Dielectric Heterostacks,” no. September, 2018.

RESEARCH PAPER 1

Effect of Temperature, Precursors concentration, and Distance between precursors on the synthesis of Molybdenum Disulfide (MoS₂) using Chemical Vapor Deposition (CVD) technique.

Aparna¹, Satakshi Pandey¹, and Bharti Singh^{1*}

¹Nanomaterial Research Laboratory, Department of Applied Physics, Delhi Technological University, Main Bawana Road, Delhi 110042, India

^{1*}Department of Applied Physics, Delhi Technological University, Main Bawana Road, Delhi 110042, India

*Corresponding Author: bhartisingh@dtu.ac.in

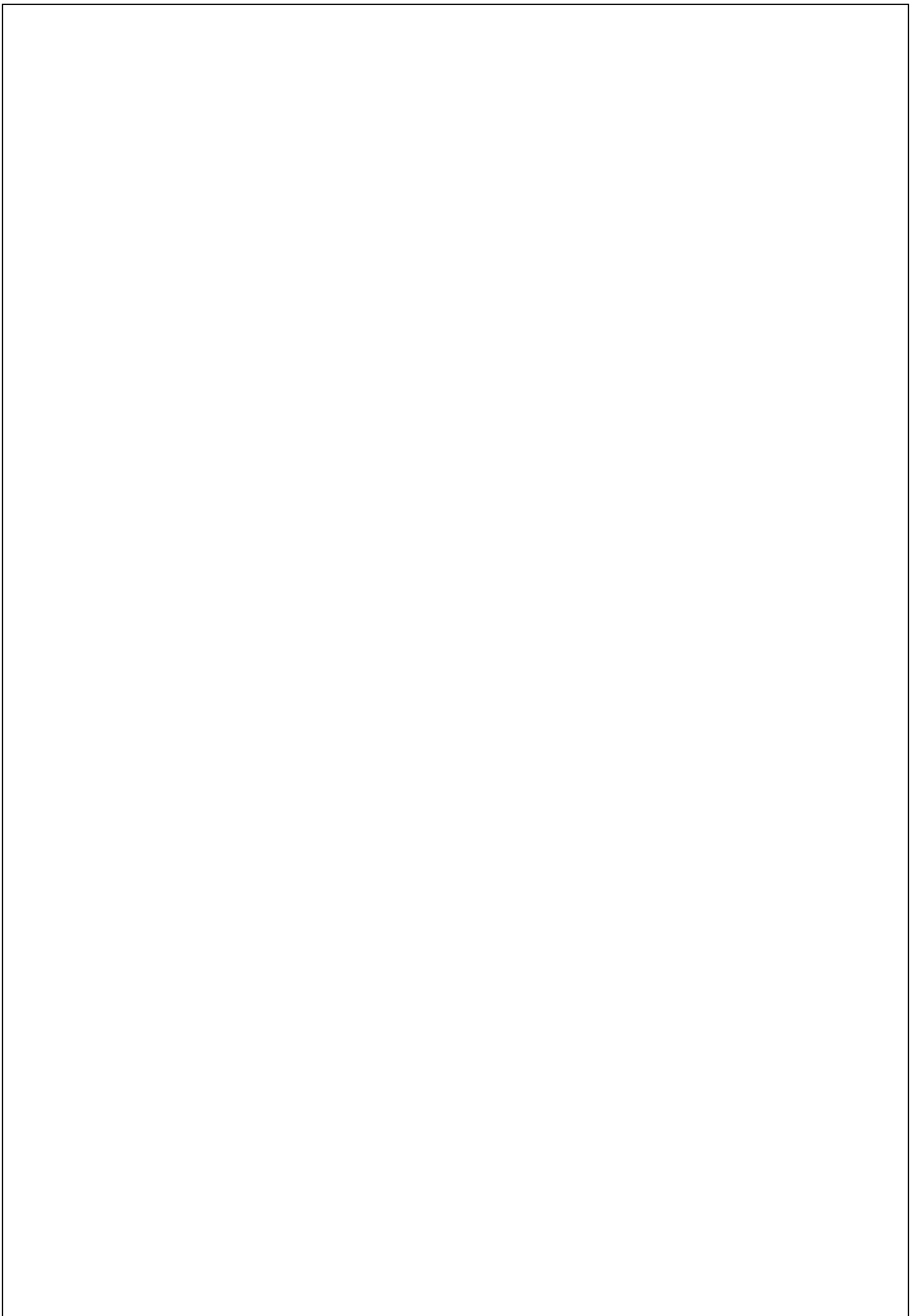
Abstract

Two-dimensional (2D) Transition Metal Dichalcogenides (TMDCs) have been engrossing a broad range of scientific interests due to their outstanding properties. Among all the explored TMDCs, MoS₂ has been eyeing the most attention. In the present study, monolayer MoS₂ has been grown on Si/SiO₂ substrate using the Chemical Vapor Deposition (CVD) technique, where MoO₃ and sulfur were used as the precursor. The sample was further studied using various characterization techniques viz. Raman Spectroscopy, and Optical Microscopy which showed that MoS₂ can be fabricated on SiO₂ substrate by maintaining the temperature at 750°C for 15 to 30 minutes.

Keywords: Transition Metal Dichalcogenides; Chemical Vapor Deposition; Optical microscope; Raman Spectroscopy.

1. Introduction

Two Dimensional layered materials such as graphene, transition metal dichalcogenides (TMDCs), hexagonal boron nitride (h-BN) have gained the attention of the scientific community due to their potential application in the field of electronic and optoelectronic devices¹. Various TMDCs that are semiconducting have been widely explored for electronic devices due to their ultrahigh mobility and semiconducting properties^{2,3}. Several groups have also investigated the enhanced optical properties of TMDCs in optoelectronic devices such as light-emitting diodes, phototransistors, and photovoltaics^{2,4,5}. The potential use of these monolayer TMDCs is due to their high absorption coefficient and direct bandgap. The application of Graphene to semiconductor devices is limited because of zero bandgap and low On/Off ratio⁶. It acts as a semi-metal and hence no longer useful for semiconductor devices⁷. MoS₂ emerged as an alternate choice over graphene because of the direct bandgap and high On/Off ratio. In literature, several methods have been carried out for the synthesis of the MoS₂, which include hydrothermal process, mechanical exfoliation, and chemical vapour deposition⁸. However, CVD has found to be the most practical methods to grow large-area TMDCs nanosheets. It has been most suitable for growing high-quality monolayer TMDCs^{9,10}. In the present study, monolayer MoS₂ has been grown using the CVD technique where MoO₃ and sulfur were used as the precursor. The results reveal that the growth temperature, precursors concentration, and distance between precursors are parameters that play a pivotal role in tuning the morphology and crystalline quality of the MoS₂ nanosheet^{11,12}. It was observed that the temperature around 750°C and the distance around 20 cm between the precursors were optimum for the monolayer growth^{13,14}. The grown triangular flakes have been characterized using Raman Spectroscopy and Optical microscopy. Two characteristic peaks E_{2g} and A_{1g} were observed at 381.8 cm⁻¹ and 401.5 cm⁻¹, respectively, with a distance of 19 cm⁻¹ indicating the monolayer nature^{8,11,12,15-17}. Tri-layer deposition of MoS₂ was also reported at the temperature around 750°C and the distance between the precursors was kept around 21 cm. As the difference between E_{2g} and A_{1g} peaks seem to increase, the monolayer is slowly moving towards the bulk nature. Optical images can also give us an idea of the layer of MoS₂ deposited on the substrate. The contrast between the substrate and the deposition increases with the number of layer.



2. Experimental Setup

MoS₂ growth on p-type <100>Si/SiO₂ substrate with oxide thickness 300 nm was carried out by using MoO₃ powder (Sigma Aldrich, 99%) and Sulfur powder (Sigma Aldrich, 99.998%) as precursors in a single zone CVD system. A diamond-tipped cutter was used to cut a 2x2 cm Si/SiO₂ substrate out of a wafer of 3-inch diameter. Substrates were first cleaned in acetone using a digital ultra-sonicator for 10 minutes. Then, the hydrophobic behaviour of the Si/SiO₂ wafer was tested under DI water, to reassure cleaning of the wafer. Argon was used as a carrier gas with a pressure of 100 sccm for the whole process.

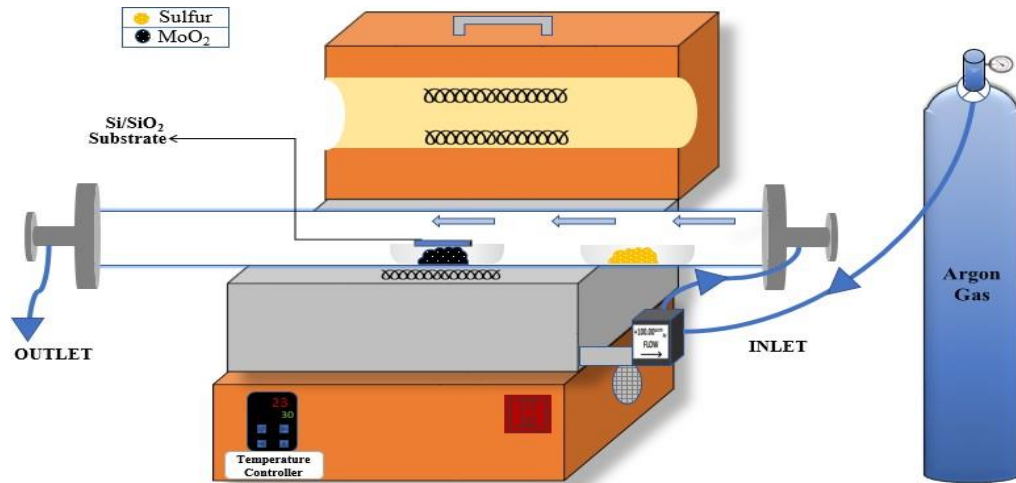


Figure 1: Diagrammatic representation of Single Zone CVD Setup.

A quartz boat holding 50 mg of MoO₃ was put in the centre of the furnace at 750°C and on the same boat, Si/SiO₂ substrate was kept facing downwards. Then at a distance of 22 cm, another quartz boat holding 200 mg of Sulfur was kept. With a ramping speed of 15°C per minute, the furnace was heated and the reaction time was set for 30 minutes. When the furnace started to cool down, the hood of the furnace was opened abruptly after few minutes and was then let to cool down at room temperature.

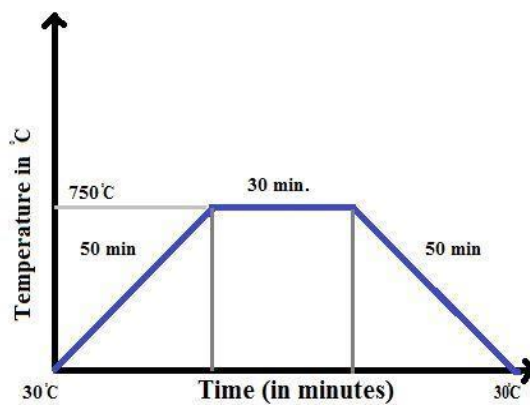


Figure 2: Profile of furnace temperature vs. Time of process.

3. Characterization

Primary judgment about the number of layers, location, and shape of the prepared samples was made using optical microscopy (Nikon Eclipse LV100) and Raman spectroscopy. The position of characteristic Raman peaks also gives us details about whether the layer deposited is monolayer or multilayer in nature.

4. Result and Discussion

4.1 Optical Spectroscopy

Optical images of the continuous thin film of MoS₂ grown on Si/SiO₂ substrate are shown in Tables 1,2,3. On observing the optical images of the triangular flakes, a lot about the number of layers can be concluded.² The growth area of the substrate is 1 cm x 1 cm, which is limited because of the small diameter of the quartz boat that was kept in CVD. On the edges of the deposited thin film, triangular flakes with edge lengths ranging from 10-45 μm were observed. Isolated triangular islands were observed of Monolayer MoS₂, whose size ranges from few microns to tens of microns. In addition to triangular islands, some other shapes like stars, and hexagons were also observed. Hexagon or merging islands are formed due to the over-deposition of MoO₂, while star shapes are seen when the temperature of the central zone of CVD was not high enough. Nucleation sites that appeared on the surface of the monolayer were resultant of the dislocation defects that occurred during the growth process¹⁸⁷. These are caused because of an excess amount of unreacted MoO₂ or excess sulfur, which created an additional site for nucleation. Owing to the longer growth/reaction time, it was found that some monolayer MoS₂ islands were overlapping with one another⁶. This resulted in the formation of bilayer and multilayer structures.

Table 1: Effect of Concentration of Precursors.

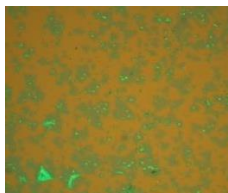
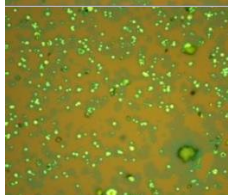

S.No	MoO ₂ (Weight in mg)	Sulfur (Weight in mg)	Distance b/w boats (in cm)	Temperature of the centre zone (in °C)	Reaction time (in minutes)	Inference	Optical Images
1.	40	160	20	750	20	Bi-layer (triangle)	
2.	20	160	20	750	20	Excess Sulfur	
3.	60	240	20	750	20	Bulk (Merging islands)	

Table 2: Effect of Distance between Boats containing Precursors

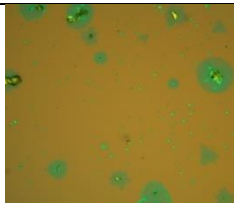
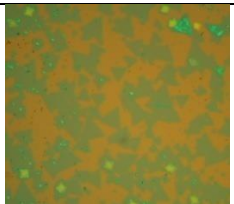
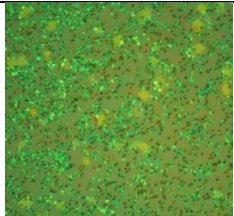
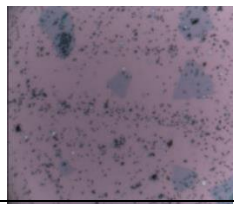

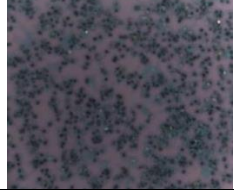
S.No.	MoO ₂ (Weight in mg)	Sulfur (Weight in mg)	Distance b/w boats (in cm)	Temperature of the centre zone (in °C)	Reaction time (in minutes)	Inference	Optical Images
1.	50	200	22	750	20	Bulk (Merging Islands)	
2.	50	200	21	750	20	Tri-Layer.	
3.	50	200	19	750	20	Bulk (Unreacted MoO ₂)	

Table 3: Effect of Temperature of the central zone of CVD

S.No.	MoO ₂ (Weight in mg)	Sulfur (Weight in mg)	Distance b/w boats (in cm)	Temperature of the center zone (in °C)	Reaction time (in minute)	Inference	Optical Images
1.	50	200	20	720	20	Bulk	
2.	50	200	20	750	20	Monolayer (triangle)	
3.	50	200	20	780	20	Bulk	

4.2 Raman Spectra

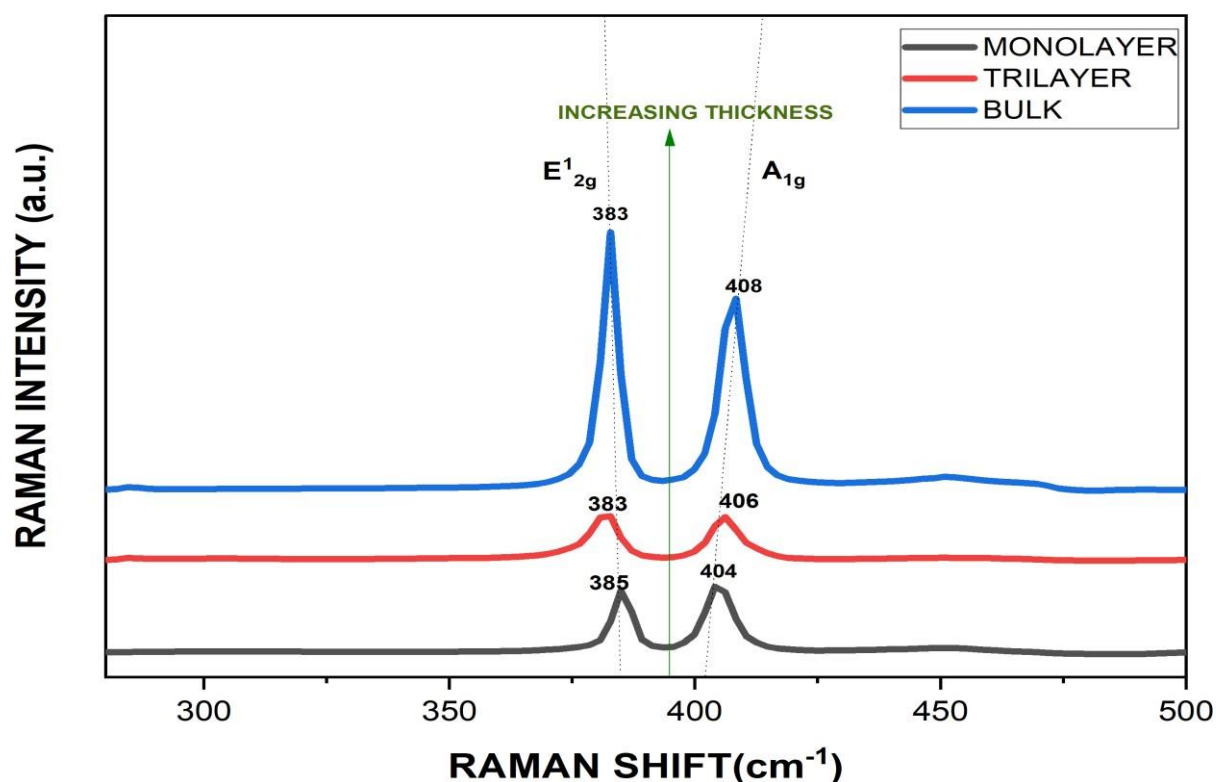


Fig. 4: Raman of MoS₂ thin film layer on SiO₂/Si showing the region with the prominent E_{2g}¹ and A_{1g} peaks.

Raman spectroscopy is a characterization tool that is used to study different crystalline structures of MoS₂. Monochromatic laser light of wavelength 532 nm is in-elastically scattered in the visible, near-infrared, or near UV region¹¹. The laser light interacts with molecular vibrations or phonons resulting in a shift in the energy of scattered light which gives details about vibrational modes in the system¹³. MoS₂ has two characteristic peaks known as E_{2g}¹ (in-plane mode) in which the two sulfur atoms vibrate in opposite directions to the molybdenum atoms and A_{1g} (out-of-plane mode) in which the two sulfur atoms vibrate in opposite directions perpendicular to the plane and the frequency difference between two indicates the number of layers¹⁹. When the number of layers reduces from multi-layer to monolayer the A_{1g} vibration mode undergoes a redshift while E_{2g}¹ vibration mode undergoes a blue shift¹⁴. In figure 4, The bulk, tri-layer, and monolayer regions show E_{2g}¹ peaks at 383 cm⁻¹, 383 cm⁻¹, 385 cm⁻¹ and A_{1g} peak at 408 cm⁻¹, 406 cm⁻¹, 404 cm⁻¹ respectively. The corresponding wavenumber difference between these two characteristic peaks is 25 cm⁻¹, 23 cm⁻¹, and 19 cm⁻¹ respectively^{9,20}. Thus, we have successfully grown large-sized, high-quality MoS₂ crystals.

5. Conclusion

In the present work, the effect of various parameters in the synthesis of the MoS₂ films on Si/SiO₂ substrate by single-zone chemical vapour deposition technique using MoO₃ and sulfur as precursors is studied. The MoS₂ films synthesized were monolayer, tri-layer, and bulk in nature, as reported by Raman Spectroscopy and Optical Microscopy. It may be highlighted that the role of concentration of precursors, the temperature of the furnace, and distance between boats carrying precursors was found to be pivotal in the desired growth of the monolayer MoS₂.

References

- ¹ H. Li, H. Wu, S. Yuan, and H. Qian, *Nat. Publ. Gr.* **1** (2016).
- ² Z. Zhu, (2019).
- ³ Z.D. Ganger, (2019).
- ⁴ D. Ma, J. Shi, Q. Ji, K. Chen, J. Yin, Y. Lin, Y. Zhang, and M. Liu, (2015).
- ⁵ R. Yang, H. Li, K.K.H. Smithe, T.R. Kim, K. Okabe, E. Pop, J.A. Fan, and H.P. Wong, *477* (2017).
- ⁶ Maiti and Bidinger, *J. Chem. Inf. Model.* **53**, 1689 (1981).
- ⁷ A.J. Boson, (2017).
- ⁸ P. Shen and M.S. Photonics, **1** (2017).
- ⁹ L.P.L. Mawlong, K.K. Paul, and P.K. Giri, *J. Phys. Chem. C* **122**, 15017 (2018).
- ¹⁰ H. Zhang, (2018).
- ¹¹ E. Rotunno, M. Bosi, L. Seravalli, G. Salviati, and F. Fabbri, *Nanoscale Adv.* **2**, 2352 (2020).
- ¹² J. Jeon, J. Lee, G. Yoo, J.H. Park, G.Y. Yeom, Y.H. Jang, and S. Lee, *Nanoscale* **8**, 16995 (2016).
- ¹³ T. Han, H. Liu, S. Wang, W. Li, S. Chen, X. Yang, and M. Cai, *Materials (Basel)*. **11**, (2018).
- ¹⁴ B. Birmingham, J. Yuan, M. Filez, D. Fu, J. Hu, J. Lou, M.O. Scully, B.M. Weckhuysen, and Z. Zhang, *ACS Appl. Nano Mater.* **1**, 6226 (2018).
- ¹⁵ Y.H. Lee, X.Q. Zhang, W. Zhang, M.T. Chang, C. Te Lin, K. Di Chang, Y.C. Yu, J.T.W. Wang, C.S. Chang, L.J. Li, and T.W. Lin, *Adv. Mater.* **24**, 2320 (2012).
- ¹⁶ L. Sun, X. Zhang, F. Liu, Y. Shen, X. Fan, S. Zheng, J.T.L. Thong, Z. Liu, S.A. Yang, and H.Y. Yang, *Sci.Rep.* **7**, 1 (2017).
- ¹⁷ M. Imran, N. Chaudhary, A.K. Hafiz, B. Singh, and M. Khanuja, *AIP Conf. Proc.* **2276**, (2020).
- ¹⁸ D. Zhu, H. Shu, F. Jiang, D. Lv, V. Asokan, and O. Omar, **1** (n.d.).
- ¹⁹ N.R. Pradhan, C. Garcia, F. Wang, Z. Wang, M.K. Francis, N. Perea-lópez, Z. Lin, N.R. Pradhan, P.M.Ajayan, H. Terrones, and L. Balicas, (2014).
- ²⁰ R. Lewandowska, H. Scientific, D. Lille, and V. Ascq, **54** (n.d.).

RESEARCH PAPER 2

Chemical Vapor Deposition grown monolayer MoS₂ based Resistive Random Access Memory Device

Satakshi Pandey¹ Aparna¹ Dr Bharti Singh^{*}

¹Nanomaterial Research Laboratory, Department of Applied Physics, Delhi Technological University, Main Bawana Road, Delhi 110042, India

^{1*}Department of Applied Physics, Delhi Technological University, Main Bawana Road, Delhi 110042, India

*Corresponding Author: bhartisingh@dtu.ac.in

Abstract: Graphene is a semimetal with zero bandgap which has imposed a limit on its applications in field-effect transistors and optoelectronics. Owing to this fact, other 2D materials such as h-BN, MXenes, phosphorene, and TMDCs were explored for their potential use in various electronic devices. Transition metal dichalcogenides (TMDCs) show excellent optical, mechanical, and electronic properties because they have a bandgap that is tunable and they exhibit a transition from indirect to direct bandgaps. Molybdenum disulfide (MoS₂) is one of the most quintessential TMDCs with a 1.84 eV direct bandgap in monolayer form which makes it scientifically as well as industrially important. Monolayer MoS₂ shows intense photoluminescence because of the quantum confinement effect. Here in this study, CVD Technique was employed for the synthesis of monolayer MoS₂ on Si/SiO₂ substrate. MoO₃ and sulfur powder were used as precursors. Several parameters including the growth temperature, precursors concentration, distance between precursors, and pressure of carrier gas were optimized for the monolayer growth. The grown film was investigated by using various characterization

techniques including Optical Microscopy, Raman Spectroscopy, and Photoluminescence spectroscopy. The results revealed that precursor concentration ($\text{MoO}_2 = 50\text{mg}$ and $\text{S} = 200\text{mg}$) at temperature 750°C and the boats containing the precursors kept at a distance of 22cm were found optimum for the monolayer growth. We have further studied the switching characteristics of the CVD-grown monolayer MoS_2 based RRAM device. Silver electrodes were deposited on the grown sample to form a planar MIM structure i.e., $\text{Ag}/\text{MoS}_2/\text{Ag}$. The typical I-V characteristics of the fabricated metal-insulator-metal (MIM) structure were studied using the two probe measurement technique.

Keywords. Non-volatile memory devices; Transition Metal Dichalcogenides; Photoluminescence spectroscopy; Raman Spectroscopy; Resistive random access memory

1 Introduction

Thin-layer two-dimensional (2D) materials, particularly monolayer MoS_2 , have unlocked new doors in the fabrication of small-scale electronic devices because of their excellent optical and electrical properties[49]. The current techniques for the fabrication of thin layers of MoS_2 include mechanical and liquid exfoliation, physical vapor deposition, and chemical vapor deposition[54]. Various scientific groups have followed multiple procedures for the good crystalline growth of monolayer MoS_2 . The chemical vapor deposition (CVD) technique is the most victorious and authentic method for large-scale and thickness-dependent growth among all the other known methods[55][23]. The growth conditions, shape and size of MoS_2 flakes are considerably dominated by factors including pressure, growth temperature, growth time, the concentration of precursors, etc.[32]. Molybdenum Disulfide (MoS_2) is an n-type semiconductor that has emerged as the most suitable contender in electronic devices. Monolayer MoS_2 which is diamagnetic undergoes a transition to direct bandgap from indirect bandgap when the layer number decreases from the bulk form to monolayer. As the number of layers increases, the bandgap decreases. Various approaches to fabricate MoS_2 include liquid intercalation, hydrothermal method, mechanical exfoliation, and chemical vapor deposition (CVD). In this study, we have overcome the challenge of synthesizing high-quality monolayer films of MoS_2 . The growth of monolayer MoS_2 films was successfully done by optimizing various parameters like concentration, reaction time, reaction temperature, pressure, and placements of boats. Field-effect transistors (FETs) based on monolayer MoS_2 have pre-eminent importance in future electronic

applications such as data storage, memory, optoelectronics, quantum optics, communication, etc. because of their high ON/OFF current ratios, their high electron-hole mobility, low operation power, and good photo-responsivity [10]. In this study, the CVD technique was used wherein MoO₂ powder and sulphur powder were used as reactants. Raman spectroscopy and photoluminescence (PL) spectroscopy were carried out to assess the optical as well as structural properties of the grown MoS₂ thin films[5]. The Raman characteristic peaks 384cm⁻¹ (E_{2g}) and 404cm⁻¹ (A_{1g}) manifest that the grown film is monolayer MoS₂[27]. A pronounced emission peak was observed at 674 nm in the photoluminescence spectrum of monolayer MoS₂[53][26]. The results revealed that we have grown monolayer MoS₂ with an optical bandgap of 1.84eV[56].

We have studied MoS₂ based devices for memory applications, and have obtained the desired result for electric switching between the semiconductor phase to the metallic phase[2]. The device was fabricated using thermal evaporation of silver onto the thin films of MoS₂ on Si/SiO₂ substrate[7]. In literature, various electrodes like tin, copper, silver, and aluminium were used for MoS₂ based memory devices[57].

The redox reaction that takes place inside MoS₂ thin films due to the easy formation of silver filament is the reason why silver is found to be the most suitable material for the fabrication of memory device[9].

Monolayer MoS₂ based memory devices show faster switching due to the high On/off ratio[6]. These RRAM devices have shown promising features because of their probable scalability, high endurance, high operation speed, and process flow ease in comparison to the flash memories[47]. RRAM is a two-terminal structure that is operated by applying a sufficiently high voltage which changes the resistance state to store information in a non-volatile manner.

2 Experimental Procedure

2.1 Fabrication of Monolayer MoS₂ thin film

Films of MoS₂ were grown on Si/SiO₂ substrate of 300 nm oxide thickness. In the Chemical vapor deposition (CVD), the precursors used were Sulphur (Sigma Aldrich, 99.98%) and Molybdenum dioxide(MoO₂) powder (Sigma Aldrich, 99.998%). The Si/SiO₂ wafer of the diameter of 3-inch was cut using a diamond cutter into dimensions of 4x4 cm. Then the substrates were cleaned using acetone for 10 minutes in the digital ultra-sonicator. To remove any remains of acetone from the surface, substrates were washed using de-ionized water[3]. The pressure of the carrier gas, i.e. Argon was kept constant at 50 sccm, throughout the whole process. The furnace was heated at a ramping speed of 15 °C per minute and the reaction time was set for 15 minutes[26]. After the reaction took place the furnace was allowed to cool down naturally to room temperature.

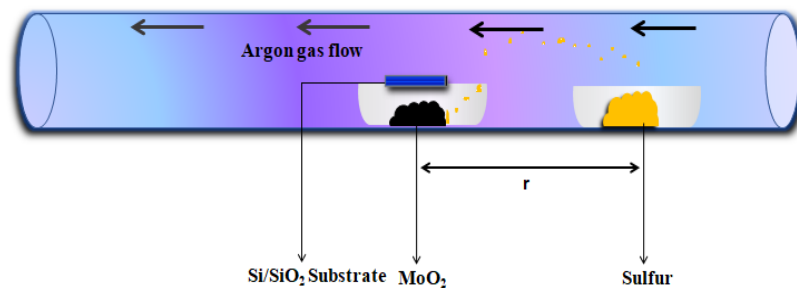


Fig. 1: Diagrammatic representation of chemical vapour disposition.

2.2 Fabrication of MoS₂ memristors

After the monolayer MoS₂ films were synthesized on the surface of thin-film Ag contacts were deposited. A common method of Physical vapor deposition is Thermal evaporation. The easy formation of silver filament due to the redox reaction was the reason why silver was found to be the most suitable material. 100 mg of Ag was evaporated in a vacuum environment to form a thin film on the MoS₂/Si/SiO₂ substrate. A lateral structure of the device was fabricated with Ag as positive and negative electrodes.

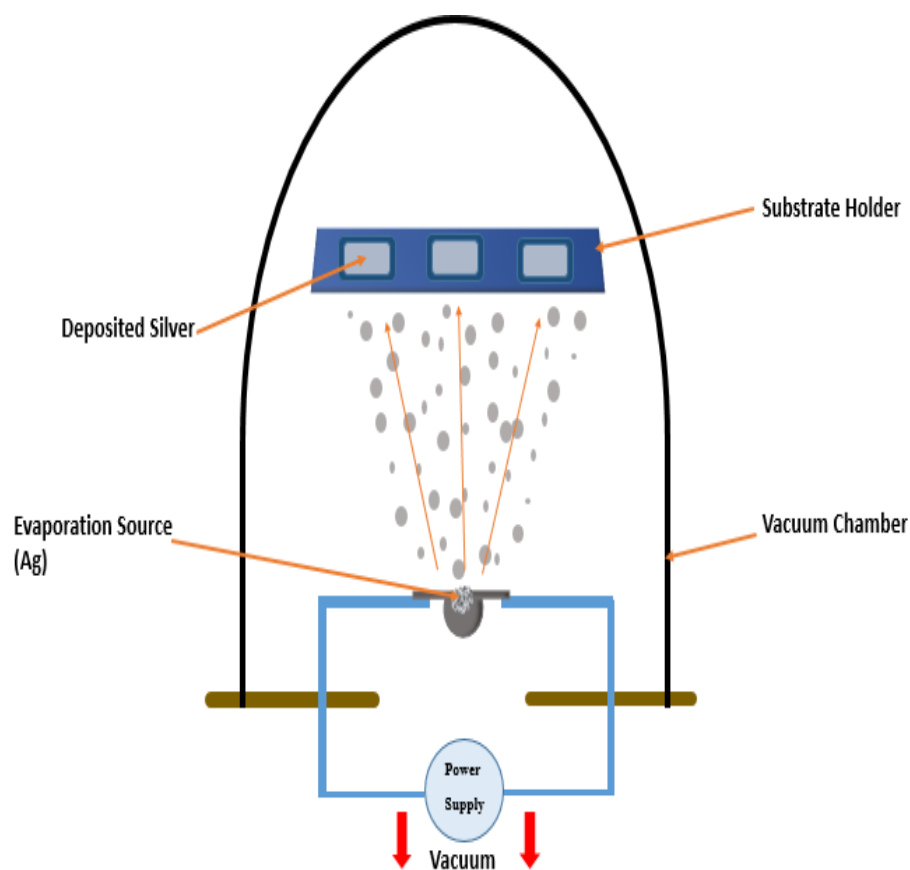
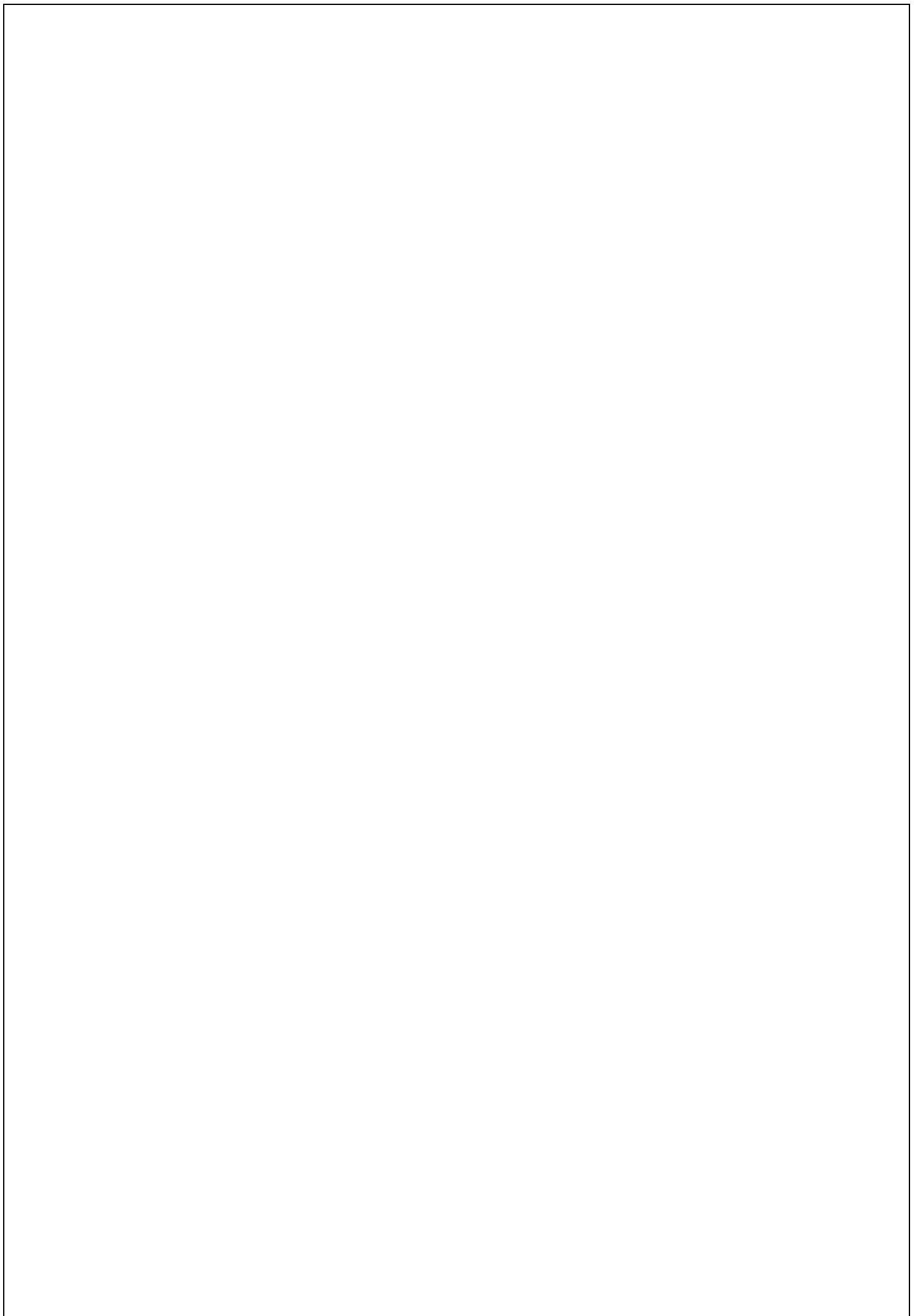


Fig. 2: Diagrammatic representation of thermal evaporation method.



3 Results and Discussion

3.1 Optical Microscopy

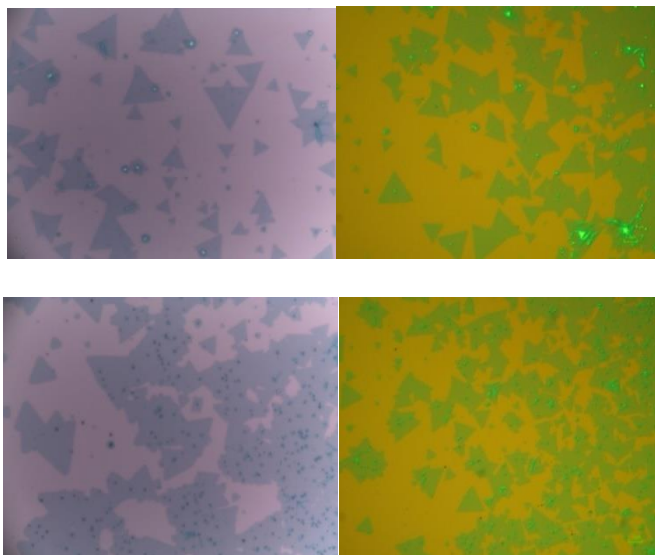


Fig. 3: Images showing a continuous thin film of MoS₂ grown on Si/SiO₂ substrate.

Triangular flakes with edge lengths ranging from 10-45 μm were observed of the deposited thin film[58]. An excess amount of unreacted MoO₂ or excess sulfur created an additional site on the surface of the monolayer MoS₂ for nucleation which caused the dislocation defects that occurred during the synthesis process[59]. When the thin film grown on the substrate was exposed to longer growth/reaction time, it was observed that few monolayer MoS₂ islands were overlapping with one another which resulted in the formation of bulk structures[51].

3.2 Photoluminescence Spectroscopy (PL)

PL measurements were done to further confirm the presence of monolayer MoS₂ using a 532 nm laser (Figure 4). Strong photoluminescence in monolayer MoS₂ is seen at the direct excitonic transition energies which are not present in the indirect bandgap bulk MoS₂ films[47]. Ground state A-exciton emission is observed when a transition occurs between the conduction band and the highest valence band at the K- points.

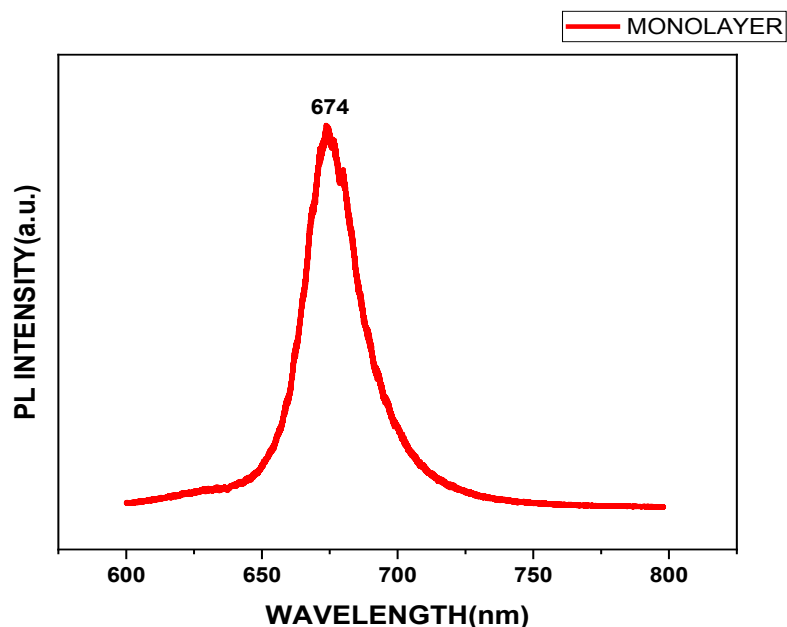
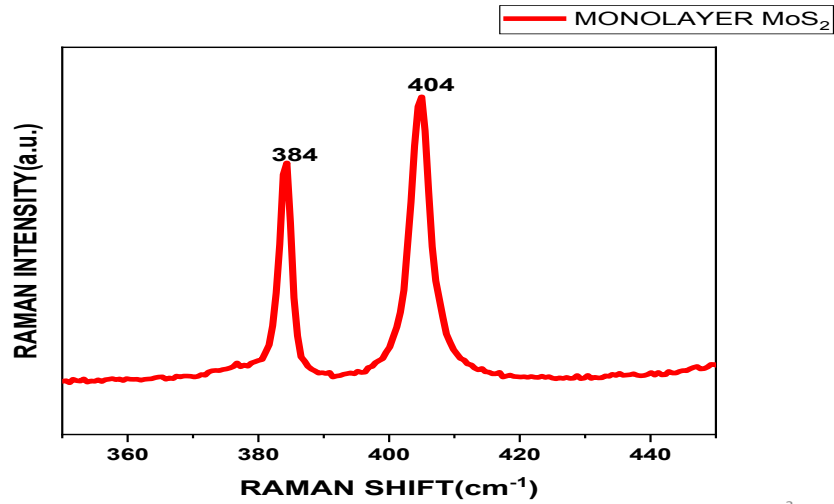


Fig. 4: Photoluminescence spectra of CVD-grown monolayer MoS₂.

This peak is observed at 674nm (1.84 eV) which appears because of the direct intraband recombination of the photo-generated electron-hole pairs. Thus from the PL spectra, we can conclude monolayer MoS₂ manifest a direct bandgap of 1.84eV[50].

3.3 Raman Spectra

In-elastic scattering of monochromatic laser light of wavelength 532 nm in the visible, near-infrared, or near UV region occurs due to interaction with molecular vibrations the outcome of which is a change in the energy of scattered light which attributes to the vibrational modes in the system[9]. Two characteristic peaks are A_{1g} (or the out-of-plane mode) in which sulfur atoms are found to be vibrating in opposite directions perpendicular to the plane and E_{2g}¹ (or the in-plane mode) in which sulfur atoms are found to be vibrating in opposite directions to the molybdenum atom are observed in the Raman spectra of MoS₂.



2

Fig. 5: For the study of different crystalline structures of MoS₂, we have used Raman spectroscopy.

The frequency difference between the two peaks is utilized to calculate the layer number in MoS₂ film. The corresponding wavenumber difference between these two characteristic peaks was observed to be 20 cm⁻¹ which indicates the monolayer nature[3].

3.4 Devices fabrication and electrical measurement

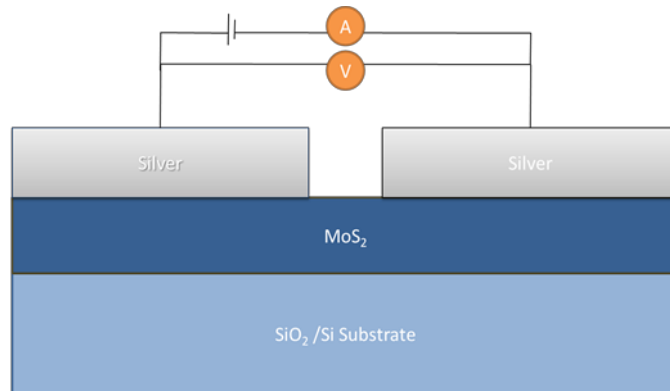


Fig.6: Electrical measurement and diagrammatic side view configurations of MoS₂ based memory device with Ag contacts.

Deposition of Ag was carried out using thermal evaporation. Keithley source meter 2450 along with the DC probe was used for the current-voltage measurement of the fabricated device.

Resistive random access memory (RRAM) devices show better performance compared to the traditional semiconductor electronic devices due to their resistive switching behaviour [8]. The advantage of using RRAM devices include plain device structure), multi-bit capability, lower energy consumption and its good compatibility which permits it to be combined into a current integrated circuit (IC) technology instead of the conventional CMOS[56]. RRAM is also deployed in neuromorphic computing as a synaptic cell and low-energy consumption computing as a non-volatile logic circuit.

RRAM is generally made up of two conductive electrodes with an insulating layer present in between forming a metal-insulator-metal structure. This structure can transition between a high-resistance state (HRS or logic 0) and a low-resistance state (LRS or logic 1) with the application of an appropriate voltage[7].The resistive-switching behaviour is divided into two types unipolar and bipolar depending on voltage polarity[9].

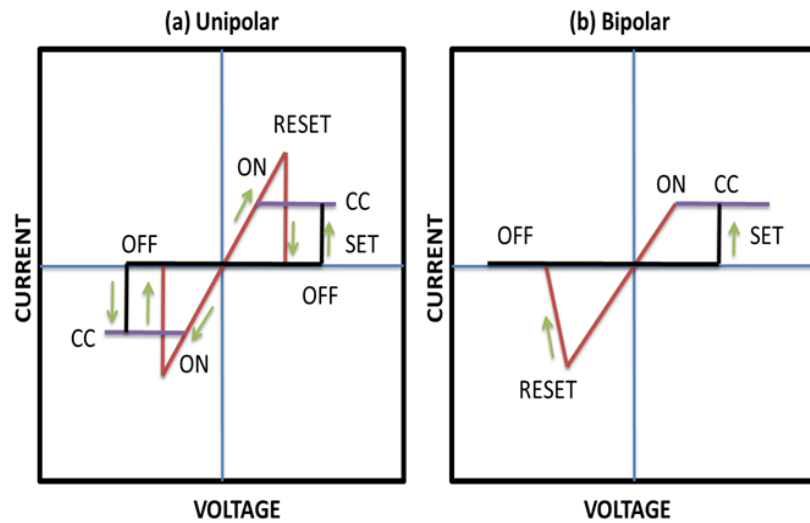


Fig.7. shows the current-voltage characteristics of devices with (a) unipolar switching and (b) bipolar switching

Resistive switching is caused by a voltage having the same polarity in the case of unipolar switching, as shown in Figure 7(a) whereas in bipolar switching, shown in Figure 7(b), one polarity is employed to transition from HRS to LRS, and the opposite polarity to change back into HRS.

The particular voltage at which the memory device transitions from ON to OFF state that means from low resistance state (LRS) to high resistance state (HRS) is referred to as RESET voltage while the switching OFF to ON state i.e., from HRS to LRS is referred to as the SET voltage. The resistive memory behaviour is explained by RESET and SET switching voltages.

The mechanism behind the Set and Reset process is the formation and the breakage of conductive filaments which causes the resistance switching (RS) in the devices. The development and the rupture usually occur at the thinnest portion of the conducting filament owing to the electrochemical dissolution or joule heating. In this study, two Ag electrodes with MoS₂ present in between define the memristor channel. Development and rupture of the conductive filament connecting the two electrodes having the monolayer MoS₂ film present in between attribute to the switching of the states[57][19].

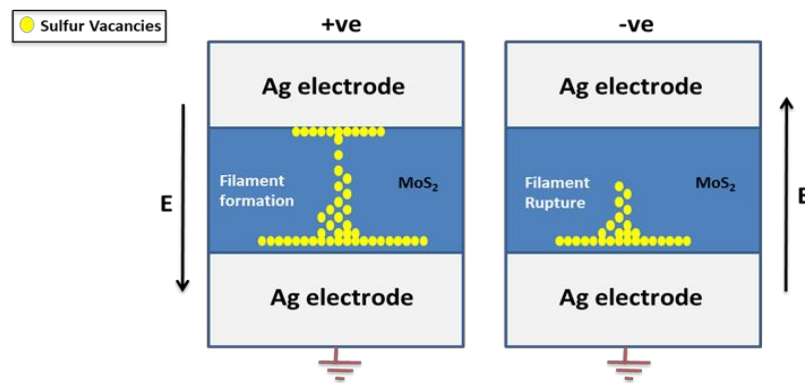


Fig. 8: Depicts the CF-type conduction mechanism in Ag/MoS₂/Ag device.

The sulfur vacancy is the principal defect in the MoS₂ monolayer but it does not provide a low-resistance path in its indigenous form[5]. However, silver ions, drifting from one electrode to the other electrode can be replaced into the sulfur vacancy, which results in a conducting local density of states (LDOS), which directs it to a low resistive state. On applying a reverse electric field Ag atoms are removed, the system goes back to a high resistive state as the defects retrieve to their initial vacancy structure[6]. At an atomic level, this switching mechanism is similar to the formation of a conductive bridge memory[57]. The silver atoms present at the positively biased electrode become positively charged silver ions after losing their electrons ($\text{Ag} \rightarrow \text{Ag}^+ + \text{e}^-$) in the SET process. These ions are attracted by the sulfur vacancies and are simultaneously reduced ($\text{Ag}^+ + \text{e}^- \rightarrow \text{Ag}$), setting up a conductive path[9]. The process in which the conductive filament connecting both the electrodes is formed is known as electroforming. ‘Electroforming’ or simply ‘forming’ is a necessary pre-treatment process in resistive switching[28]. The application of either a voltage or a current leads to the development of conductive filament and consequently decreasing the cell’s resistance[8].

Now if we apply a voltage sweep, cell's resistance can decrease drastically at a certain voltage which causes a large increase in the power dissipation[57]. This can destroy the cell and cause dielectric breakdown[28].

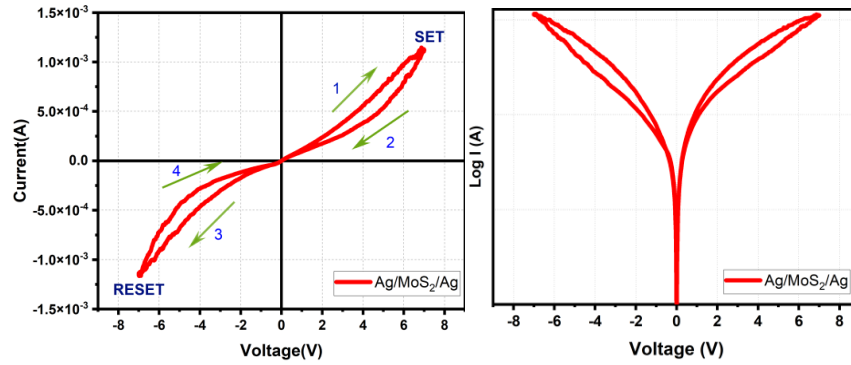


Fig. 9: (a) linear plot and (b) semi-logarithmic plot for the same two-probe transfer characteristics for a typical Ag/MoS₂/Ag device. The voltage was swept in the sequence of 0 V → 7V → 0 V → -7 V → 0 V, as shown by the coloured arrows with the four sweeps labelled as 1, 2, 3 and 4.

Dielectric breakdown causes an indefinite decrease in the cell's resistance which makes the transition back to the HRS not possible[56]. To avoid such a situation a current compliance function is provided that can manage the maximum current (known as compliance current) flowing in the cell. D.C. electrical measurements were performed on the prepared Ag/MoS₂/Ag device configuration by sweeping the tip bias[8][2][26]. It is observed that the device manifest bipolar switching[28].

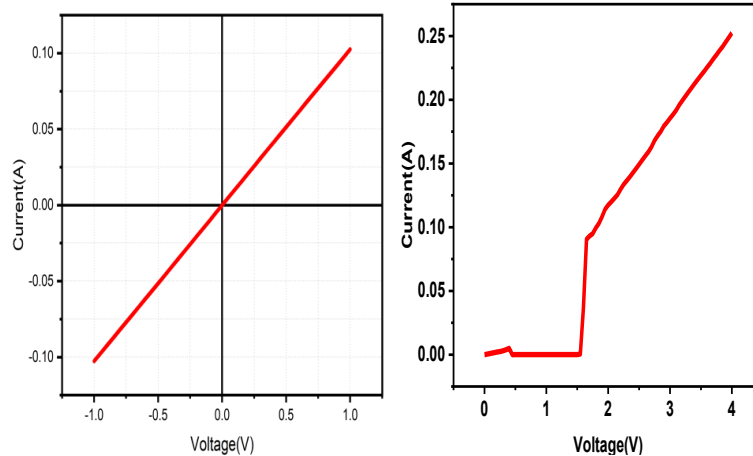


Fig.10: (a) Two similar contacts configuration of both electrodes causes the current-voltage curves to be symmetric around the zero bias (b) Set switching is exhibited by Threshold switching which at a certain voltage (V_{set}) leads to the low resistance state which can be retained till a certain voltage (V_{reset}) is lower than the applied voltage.

4 Conclusions

In summary, Monolayer MoS₂ film was grown on 300nm SiO₂/Si substrate via the CVD technique. The presence of monolayer film was attested by optical microscopy, Raman spectroscopy, and Photoluminescence Spectroscopy. Further, we have explained the resistive switching mechanism in Ag/MoS₂/Ag memory device. The formation/rupture of conductive filament has been demonstrated elaborately for the prepared device. The fabricated Ag/MoS₂/Ag memory device exhibits a bipolar resistive switching phenomenon. This study opens more doors for RRAM devices in future non-volatile memory applications.

References

- [1] A. Manuscript, "Nanoscale," 2017, doi: 10.1039/C7NR01755C.
- [2] R. Xu *et al.*, "Vertical MoS₂ Double-Layer Memristor with Electrochemical Metallization as an Atomic-Scale Synapse with Switching Thresholds Approaching 100 mV," *Nano Lett.*, vol. 19, no. 4, pp. 2411–2417, 2019, doi: 10.1021/acs.nanolett.8b05140.
- [3] M. Imran, N. Chaudhary, A. K. Hafiz, B. Singh, and M. Khanuja, "CVD synthesis and characterization of ultrathin MoS₂ film," *AIP Conf. Proc.*, vol. 2276, no. October, 2020, doi: 10.1063/5.0026128.
- [4] Y. H. Lee *et al.*, "Synthesis of large-area MoS₂ atomic layers with chemical vapor deposition," *Adv. Mater.*, vol. 24, no. 17, pp. 2320–2325, 2012, doi: 10.1002/adma.201104798.
- [5] A. Splendiani *et al.*, "Emerging photoluminescence in monolayer MoS₂," *Nano Lett.*, vol. 10, no. 4, pp. 1271–1275, 2010, doi: 10.1021/nl903868w.
- [6] J. C. Scott and L. D. Bozano, "Nonvolatile memory elements based on organic materials," *Adv. Mater.*, vol. 19, no. 11, pp. 1452–1463, 2007, doi: 10.1002/adma.200602564.
- [7] M. M. Rehman *et al.*, "Decade of 2D-materials-based RRAM devices : a review Decade of 2D-materials-based RRAM devices : a review," *Sci. Technol. Adv. Mater.*, vol. 21, no. 1, pp. 147–186, 2020, doi: 10.1080/14686996.2020.1730236.
- [8] S. Yu, R. Jeyasingh, Y. Wu, and H. S. Philip Wong, "Understanding the conduction and switching mechanism of metal oxide RRAM through low frequency noise and AC conductance measurement and analysis," *Tech. Dig. - Int. Electron Devices Meet. IEDM*, pp. 275–278, 2011, doi: 10.1109/IEDM.2011.6131537.
- [9] X. Zhao *et al.*, "Reversible alternation between bipolar and unipolar resistive switching in Ag/MoS₂/Au structure for multilevel flexible memory," *J. Mater. Chem. C*, vol. 6, no. 27, pp. 7195–7200, 2018, doi: 10.1039/c8tc01844h.
- [10] T. Han *et al.*, "Research on the factors affecting the growth of large-size monolayer MoS₂ by APCVD," *Materials (Basel)*, vol. 11, no. 12, 2018, doi: 10.3390/ma11122562.
- [11] Y. Lee *et al.*, "Synthesis of wafer-scale uniform molybdenum disulfide films with control over the layer number using a gas phase sulfur precursor," *Nanoscale*, vol. 6, no. 5, pp. 2821–2826, 2014, doi: 10.1039/c3nr05993f.

- [12] J. T. Han *et al.*, “Extremely efficient liquid exfoliation and dispersion of layered materials by unusual acoustic cavitation,” *Sci. Rep.*, vol. 4, pp. 1–7, 2014, doi: 10.1038/srep05133.
- [13] S. J. Kim *et al.*, “Large-scale Growth and Simultaneous Doping of Molybdenum Disulfide Nanosheets,” *Sci. Rep.*, vol. 6, no. October 2015, pp. 1–7, 2016, doi: 10.1038/srep24054.
- [14] S. H. Choi *et al.*, “Water-Assisted Synthesis of Molybdenum Disulfide Film with Single Organic Liquid Precursor,” *Sci. Rep.*, vol. 7, no. 1, pp. 1–8, 2017, doi: 10.1038/s41598-017-02228-8.
- [15] Z. Lin *et al.*, “Solution-processable 2D semiconductors for high-performance large-area electronics,” *Nature*, vol. 562, no. 7726, pp. 254–258, 2018, doi: 10.1038/s41586-018-0574-4.
- [16] X. Tan, W. Kang, J. Liu, and C. Zhang, “Synergistic Exfoliation of MoS₂ by Ultrasound Sonication in a Supercritical Fluid Based Complex Solvent,” *Nanoscale Res. Lett.*, vol. 14, no. 1, 2019, doi: 10.1186/s11671-019-3126-4.
- [17] H. Kim *et al.*, “Sulfidation characteristics of amorphous nonstoichiometric Mo-oxides for MoS₂ synthesis,” *Appl. Surf. Sci.*, vol. 535, no. April 2020, p. 147684, 2021, doi: 10.1016/j.apsusc.2020.147684.
- [18] O. Samy, S. Zeng, M. D. Birowosuto, and A. El Moutaouakil, “A Review on MoS₂ Properties , Synthesis , Sensing Applications and Challenges,” pp. 1–24, 2021.
- [19] D. Zhu, H. Shu, F. Jiang, D. Lv, V. Asokan, and O. Omar, “Capture the growth kinetics of CVD growth of two-dimensional MoS₂,” pp. 1–24.
- [20] D. Ma *et al.*, “A universal etching-free transfer of MoS₂ films for applications in photodetectors,” 2015, doi: 10.1007/s12274-015-0866-z.
- [21] X. Wang, H. Tian, H. Zhao, T. Zhang, and W. Mao, “Interface Engineering with MoS₂ – Pd Nanoparticles Hybrid Structure for a Low Voltage Resistive Switching Memory,” vol. 1702525, pp. 1–8, 2017, doi: 10.1002/sml.201702525.
- [22] A. A. Bessonov, M. N. Kirikova, D. I. Petukhov, M. Allen, T. Ryhänen, and M. J. A. Bailey, “Layered memristive and memcapacitive switches for printable electronics,” no. November, 2014, doi: 10.1038/NMAT4135.
- [23] L. Sun *et al.*, “Vacuum level dependent photoluminescence in chemical vapor deposition-grown monolayer MoS₂,” *Sci. Rep.*, vol. 7, no. 1, pp. 1–9, 2017, doi: 10.1038/s41598-017-15577-1.
- [24] W. Wang, G. N. Panin, X. Fu, L. Zhang, and P. Ilanchezhian, “MoS₂ memristor with photoresistive switching,” no. July, pp. 1–10, 2016, doi: 10.1038/srep31224.
- [25] L. P. L. Mawlong, K. K. Paul, and P. K. Giri, “Direct Chemical Vapor Deposition Growth of Monolayer MoS₂ on TiO₂ Nanorods and Evidence for Doping-Induced Strong Photoluminescence Enhancement,” *J. Phys. Chem. C*, vol. 122, pp. 15017–15025, 2018, doi: 10.1021/acs.jpcc.8b03957.
- [26] N. R. Pradhan *et al.*, “CVD-grown monolayered MoS₂ as an effective photosensor operating at low-voltage counter electrodes CVD-grown monolayered MoS₂ as an effective photosensor operating at low-voltage,” 2014, doi: 10.1088/2053-1583/1/1/011004.
- [27] J. Chen *et al.*, “Chemical Vapor Deposition of High-Quality Large-Sized MoS₂ Crystals on Silicon Dioxide Substrates,” no. March, 2016, doi: 10.1002/advs.201600033.
- [28] F. Zahoor, T. Z. Azni Zulkifli, and F. A. Khanday, “Resistive Random Access Memory (RRAM): an Overview of Materials, Switching

- Mechanism, Performance, Multilevel Cell (mlc) Storage, Modeling, and Applications,” *Nanoscale Res. Lett.*, vol. 15, no. 1, 2020, doi: 10.1186/s11671-020-03299-9.
- [29] J. Liu, Z. Zeng, X. Cao, G. Lu, L. Wang, and Q. Fan, “Preparation of MoS₂-Polyvinylpyrrolidone Nanocomposites for Flexible Nonvolatile Rewritable Memory Devices with Reduced Graphene Oxide Electrodes,” pp. 1–6, 2012, doi: 10.1002/sml.201200999.
- [30] V. K. Sangwan *et al.*, “Gate-tunable memristive phenomena mediated by grain boundaries in single-layer MoS₂,” *Nat. Nanotechnol.*, vol. 10, no. 5, pp. 403–406, 2015, doi: 10.1038/nnano.2015.56.
- [31] P. Cheng, K. Sun, and Y. H. Hu, “Memristive Behavior and Ideal Memristor of 1T Phase MoS₂ Nanosheets,” 2015, doi: 10.1021/acs.nanolett.5b04260.
- [32] P. Yang *et al.*, “Batch production of 6-inch uniform monolayer molybdenum disulfide catalyzed by sodium in glass,” *Nat. Commun.*, no. 2018, pp. 1–10, doi: 10.1038/s41467-018-03388-5.
- [33] M. M. Rehman, G. U. Siddiqui, J. Z. Gul, and S. Kim, “Resistive Switching in All-Printed, Flexible and Hybrid MoS₂-PVA Nanocomposite based Memristive Device Fabricated by Reverse Offset,” *Nat. Publ. Gr.*, no. June, pp. 1–10, 2016, doi: 10.1038/srep36195.
- [34] Y. Xia *et al.*, “Metal ion formed conductive filaments by redox process induced nonvolatile resistive switching memories in MoS₂ film,” *Appl. Surf. Sci.*, 2017, doi: 10.1016/j.apsusc.2017.07.257.
- [35] H. Search *et al.*, “ce pte d M us pt,” 2017.
- [36] D. Wang, F. Ji, X. Chen, Y. Li, B. Ding, and Y. Zhang, “device Quantum conductance in MoS₂ quantum dots-based nonvolatile resistive memory device,” vol. 093501, 2017, doi: 10.1063/1.4977488.
- [37] L. Guan *et al.*, “Thiol-modified MoS₂ nanosheets as a functional layer for electrical bistable devices,” no. April, 2017, doi: 10.1016/j.optcom.2017.07.035.
- [38] P. Chen *et al.*, “An RRAM with a 2D Material Embedded Double Switching Layer for Neuromorphic Computing,” *2018 IEEE 13th Nanotechnol. Mater. Devices Conf.*, vol. 1, pp. 1–4, 2018, doi: 10.1109/NMDC.2018.8605915.
- [39] X. Liang, “MoS₂ Memristors Exhibiting Variable Switching Characteristics towards Bio-Realistic Synaptic Emulation,” 2018, doi: 10.1021/acsnano.8b03977.
- [40] X. Feng *et al.*, “T8-4 First Demonstration of a Fully-Printed MoS₂ RRAM on Flexible Substrate with Ultra-Low Switching Voltage and its Application as Electronic Synapse T88 T89,” *2019 Symp. VLSI Technol.*, pp. T88–T89, 2019.
- [41] M. Graf *et al.*, *Fabrication and practical applications of molybdenum disulfide nanopores*. Springer US.
- [42] M. S. Kadhim *et al.*, “Existence of Resistive Switching Memory and Negative Differential Resistance State in Self-Colored MoS₂/ZnO Heterojunction Devices,” *ACS Appl. Electron. Mater.*, vol. 1, pp. 318–324, 2019, doi: 10.1021/acsaelm.8b00070.
- [43] A. Kumar, S. Pawar, S. Sharma, and D. Kaur, “Bipolar resistive switching behavior in MoS₂ nanosheets fabricated on ferromagnetic shape memory alloy,” vol. 262106, 2018, doi: 10.1063/1.5037139.
- [44] M. U. Heterostructure *et al.*, “Infrared-Sensitive Memory Based on Direct-

- Grown,” vol. 1803563, pp. 1–9, 2018, doi: 10.1002/adma.201803563.
- [45] M. Kim *et al.*, “Zero-static power radio-frequency switches based on MoS₂ atomrlistors,” *Nat. Commun.*, no. 2018, pp. 1–7, doi: 10.1038/s41467-018-04934-x.
- [46] Q. Wang *et al.*, “Nonvolatile infrared memory in MoS₂ / PbS van der Waals heterostructures,” no. April, pp. 1–8, 2018.
- [47] B. Birmingham *et al.*, “Spatially-Resolved Photoluminescence of Monolayer MoS₂ under Controlled Environment for Ambient Optoelectronic Applications,” *ACS Appl. Nano Mater.*, vol. 1, no. 11, pp. 6226–6235, 2018, doi: 10.1021/acsnm.8b01422.
- [48] H. Van Ngoc, Y. Qian, S. K. Han, and D. J. Kang, “PMMA-Etching-Free Transfer of Wafer-scale Chemical Vapor Deposition Two-dimensional Atomic Crystal by a Water Soluble Polyvinyl Alcohol Polymer Method,” *Nat. Publ. Gr.*, no. August, pp. 1–9, 2016, doi: 10.1038/srep33096.
- [49] R. Yang *et al.*, “2D Molybdenum Disulfide (MoS₂) Transistors Driving RRAMs with 1T1R Configuration,” pp. 477–480, 2017, doi: 10.1021/acsnano.7b04100.
- [50] J. Wang *et al.*, “Magnetic field controllable nonvolatile resistive switching effect in silicon device,” *Appl. Phys. Lett.*, vol. 104, no. 24, 2014, doi: 10.1063/1.4884771.
- [51] Maiti and Bidinger, “~~濟無~~No Title No Title,” *J. Chem. Inf. Model.*, vol. 53, no. 9, pp. 1689–1699, 1981.
- [52] P. Shen and M. S. Photonics, “Large-area CVD Growth of Two-dimensional Transition Metal Dichalcogenides and Monolayer MoS₂ and WS₂ Metal – oxide – semiconductor Field-effect Transistors by Master of Science in Electrical Engineering,” pp. 1–55, 2017.
- [53] R. Lewandowska, H. Scientific, D. Lille, and V. Ascq, “Number of layers of MoS₂ determined using Raman Spectroscopy,” pp. 54–55.
- [54] D. Falola and I. Suni, “Electrodeposition of MoS₂ for Charge Storage in Electrochemical Supercapacitors,” vol. 9, no. 9, 2016, doi: 10.1149/2.0011610jes.This.
- [55] Z. D. Ganger, “Growth of Two-Dimensional Molybdenum Disulfide via Chemical Vapor Deposition GROWTH OF TWO-DIMENSIONAL MOLYBDENUM,” 2019.
- [56] K. Thakar and S. Lodha, “Optoelectronic and photonic devices based on transition metal dichalcogenides,” *Mater. Res. Express*, vol. 7, no. 1, 2019, doi: 10.1088/2053-1591/ab5c9c.
- [57] Z. Shen, C. Zhao, Y. Qi, I. Z. Mitrovic, and L. Yang, “Memristive Non-Volatile Memory Based on Graphene Materials.”
- [58] E. Rotunno, M. Bosi, L. Seravalli, G. Salviati, and F. Fabbri, “Influence of organic promoter gradient on the MoS₂ growth dynamics,” *Nanoscale Adv.*, vol. 2, no. 6, pp. 2352–2362, 2020, doi: 10.1039/d0na00147c.
- [59] H. Zhang, “Nucleation and Growth Mechanisms of 2D Semiconductor / high- ϵ Dielectric Heterostacks,” no. September, 2018.